ROLES OF CALCIUM IONS AND CYCLIC AMP IN OLFACTORY TRANSDUCTION

DISSERTATION

Presented to the Graduate Council of the
North Texas State University in Partial
Fulfillment of the Requirements

For the Degree of

DOCTOR OF PHILOSOPHY

By

Bruce D. Winegar, B.A., M.A.
Denton, Texas
December 1986

Winegar, Bruce D., Roles of Calcium Ions and Cyclic AMP in Olfactory Transduction. Doctor of Philosophy (Biological Sciences) December 1986, 102 pp., 3 tables, 22 illustrations, bibliography, 92 titles.

The roles of Ca^{2+} and cAMP in olfactory transduction were explored using agents which affect calcium channels and second messenger systems. These agents were applied at certain calculated final concentrations onto olfactory epithelia of urethane-anesthetized frogs (Rana pipiens) by two-sec aerosol spray. During extracellular recording, saturated vapors of isoamyl acetate were delivered every 100 sec in 0.3 sec pulses to produce an electroolfactogram (EOG).

Inorganic cations that block inward calcium currents inhibit EOG responses with the following rank order:

$(La^{3+}) > (Zn^{2+}, Cd^{2+}) > (Al^{3+}, Ca^{2+}, Sr^{2+}) > (Co^{2+})$.

Application of 7.5 mM La^{3+} eradicates EOG's, while Ba^{2+} (which can carry more current that Ca^{2+}) initially produces significant enhancement ($F=43.04$, $p<0.001$, $df=19$). Magnesium ion has no effect on EOG's at 7.5 mM, while 1.5×10^{-4}M Ca^{2+} is significantly inhibitory ($F=5.74$; $p=0.0355$; $df=12$). Control aerosol sprays of distilled water depress EOG's by an average of 5%.

The organic calcium channel antagonists diltiazem and verapamil inhibit EOG's by 17% and 36%, respectively, at a concentration of 1.5×10^{-4}M. Verapamil produces significant

inhibition ($F=17.17$; $p=0.002$; $df=11$) at 1.5×10^{-5}M, while the 1,4-dihydropyridine calcium channel antagonists, nicardipine and nifedipine, do not inhibit beyond 1% DMSO controls.

Several calmodulin antagonists decrease EOG's, but without correlation to their anti-calmodulin potency. Application of 1.5×10^{-4}M chlorpromazine and N-(6-aminohexyl)-5-chloro-1-naphthalenesulfonamide inhibit EOG's by 31% and 27%, respectively, while trifluoperazine inhibits by 23%.

Dibutyryl cAMP, a lipophilic mimic of cAMP, produces 54% inhibition at 1.5×10^{-4}M. Dibutyryl cGMP, cGMP, cAMP, and adenosine all decrease EOG's by less than 15% compared to distilled water controls. Forskolin, a reversible activator of adenylate cyclase, inhibits EOG's by 57% at 1.5×10^{-5}M, which is significant beyond the 1% DMSO controls ($F=17.17$; $p=0.002$; $df=11$).

These data support the hypothesis that Ca^{2+} participates in olfactory transduction. Calcium ions could serve as charge carriers, second messengers, or both. Cyclic AMP could be involved with the primary excitatory process or sensory adaptation, or both.

TABLE OF CONTENTS

LIST OF TABLES

LIST OF ILLUSTRATIONS

CHAPTER I

INTRODUCTION

Olfactory Receptor Neurons

Vertebrate olfactory transduction takes place in the olfactory epithelium. Both olfactory receptor neurons and free nerve endings of the trigeminal nerve located in the olfactory epithelium respond to odorants (Silver and Maruniak, 1981). Supporting cells in the epithelium form a matrix in which the receptor neurons are dispersed (Graziadei and Graziadei, 1976). Olfactory receptor neurons undergo constant turnover (Graziadei, 1973). They differentiate from a stem cell population and send unmyelinated axons to synapse on mitral, tufted, and periglomerular cell dendrites in the olfactory bulb (Shepherd, 1974). These axons exhibit slow spike discharge rates in the absence of any stimulus and increase or decrease their firing rate after exposure to various odorants (Gesteland et al., 1965). Unlike other sensory receptors, olfactory neurons receive no centrifugal inputs from the central nervous system (Gesteland et al., 1965).

The olfactory receptor neuron is a bipolar primary sensory neuron possessing a single apical dendrite which bears cilia. These olfactory cilia exhibit a regular 9+2

pattern of microtubules (Barber, 1974) and vary in number and length across species. In the frog, there are typically five or six cilia per neuron (Reese, 1965) with an average length of 30 μm, but they can extend up to 200 μm (Getchell et al., 1980). Olfactory cilia are about 0.25 μm in diameter and taper to 0.15 μm at the distal tip (Lancet, 1986). Proximal segments of olfactory cilia in the frog contain dynein arms and have motility (Lidow et al., 1983). Mature olfactory cilia of mammals lack dynein arms and are nonmotile (Lancet, 1986).

The cilia are necessary for olfactory transduction (De Simone, 1981; Adamek et al., 1984), probably because they contain membrane receptor sites which bind specific odorant molecules. Menco et al. (1976) have observed high densities of intramembranous particles at the distal ends of bovine and mouse olfactory cilia, which they suggest may harbor the receptor sites. Using an isolated cilia preparation from the rainbow trout Salmo gairdneri, Rhein and Cagan (1980) observed specific binding of radioactively labeled odorants (the amino acids L-alanine, D-alanine, L-lysine, L-serine, and L-threonine).

Olfactory neurons also appear to have specific binding sites for neurotransmitters (Hirsch and Margolis, 1981). Shepherd and Hedlund (1983) reported the presence of muscarinic receptors in salamander olfactory epithelium, possibly located on olfactory receptor neurons. Anholt et

al. (1984) demonstrated peripheral-type benzodiazepine receptors are present in the mouse olfactory mucosa and olfactory bulb with higher receptor densities than in other tissues. The relevence of neurotransmitter binding sites to olfactory transduction is presently unknown, although Anholt et al. (1984) speculate that peripheral-type benzodiazepine receptors may be involved in receptor cell growth and differentiation.

The Transduction Process in Olfaction

Olfactory transduction likely begins when odorant molecules bind to receptors on olfactory receptor neurons or their cilia (Menco et al., 1976). Odorant-receptor binding presumably affects the functional state of ion channels by mechanisms similar to those which mediate the actions of chemical messengers such as neurotransmitters or hormones. These mechanisms may include: (1) conformational changes induced by messenger binding to a recognition site on a receptor/ionophore (Karlin, 1983), including receptor-operated ion channels (Hurwitz, 1986); (2) modulation of ion channel conductance via protein phosphorylation by second messengers such as adenosine 3':5'-cyclic monophosphate (cAMP) (DePeyer et al., 1982; Takai et al., 1982; Levitan et al., 1983) or calmodulin

(Cohen, 1982); (3) mobilization of Ca^{2+} and activation of protein kinase C by the signal-dependent breakdown of inositol phospholipids (Fisher et al., 1984; Nishizuka, 1984).

While Na^{+} currents are regarded as the primary source of the receptor potential (Lancet, 1986), the experimental literature is sparse on the question of the ions involved in olfactory transduction. At least two other studies have implicated Ca^{2+}, although the authors may not have fully understood the significance of their data at the time.

Suzuki (1978) observed that in the lamprey, La^{3+} or Co^{2+} (calcium channel blockers) or EGTA (a calcium chelator) blocked spike responses to L-arginine, while changes in Na^{+} and K^{+} concentration had no effect. Takagi et al. (1969) observed decreases in frog EOG amplitudes upon replacing Na^{+} with divalent cations now known to block Ca^{2+} channels. However, replacement of Na^{+} with Li^{+}, which is nearly as permeant as Na^{+}, did not support EOG responses. When Na^{+} was replaced with Sr^{2+}, which is highly permeable through calcium channels, EOG's continued to be elicited at a reduced amplitude while replacement with Zn^{2+} eliminated EOG's (Takagi et al., 1969).

Recently an odorant-sensitive potassium channel has been partially characterized. Working with artificial membranes from rat olfactory epithelial homogenates, Vodyanoy and Murphy (1983) observed that chemosensitive

single channel activity can be blocked by 4-aminopyridine, a potassium channel blocker. Additionally, Dionne (1986) recorded outward currents from K^+-selective channels in dissociated Necturus (mud puppy) olfactory receptor cells. However, K^+ currents were not elicited after exposure to odorants. Clearly, further work is needed to characterize the ionic selectivity of membrane channels and their role in olfactory receptor potential generation.

Olfactory Receptor Potentials

Receptor potentials from the spatial summation of the responses of many olfactory neurons can be routinely recorded en masse using the electroolfactogram (EOG) method (Ottoson, 1956). With this method a Ringer/agar-filled capillary electrode is placed on the surface of the mucosa. The EOG response is a surface-negative potential of as much as 5 mV in the frog and may last for several seconds. In some cases a brief positive-going event occurs before the main negative-going wave (Gesteland, 1964). These EOG's occasionally have oscillatory potentials superposed on the mid-point of the main wave. They form a brief train of sine wave-like oscillations with about a 50 msec period. While the origin of the oscillations is unknown, they are widely regarded as an artifact of high stimulus levels. A recovery

phase follows these events in the form of a slow return to baseline.

The latency for spike responses after odorant presentation lasts from 45-2,000 msec, decreasing with increased odorant concentration (Getchell et al., 1980). Other sensory receptors do not exhibit such a long latency (Fuortes, 1971), supporting the hypothesis of Getchell et al. (1980) that the latency is due to odorant diffusion within the mucous. However, Libet (1970) reports that response latencies last a comparable 200-300 msec in superior cervical ganglion neurons. Muscarinic cholinergic receptors appear to mediate these responses. These receptors initiate slow excitatory postsynaptic potentials (EPSP's) that are also of comparable duration with EOG waveforms. Superior cervical ganglia also sometimes produce oscillatory potentials (Libet, 1967) that appear similar to those recorded from olfactory neurons. These parallels suggest that odorant receptors may be coupled to ion channels through second messenger systems such as those connected with muscarinic receptors. Nevertheless, the mechanism of spike latencies in olfaction is still an open question, with a leading hypothesis that olfactory transduction is linked to inherently slow cellular relay mechanisms such as those apparently responsible for long latencies in the superior cervical ganglion.

Calcium Channels and Olfactory Transduction

All excitable cells appear to possess calcium channels in the lipid bilayer of the membrane (Hille, 1984). Membrane calcium currents can be blocked by certain multivalent cations, such as the following, listed in order of decreasing potency: La^{3+}, Cd^{2+}, Zn^{2+}, Co^{2+}, Ni^{2+}, Mn^{2+}, Ca^{2+}, Sr^{2+}, and Mg^{2+} (Hagiwara and Takahashi, 1967; Hagiwara and Byerly, 1983). Lanthanum ion, a particularly effective channel blocker, binds to a site on the outer mouth of calcium channels (Glossmann et al., 1982). All of these cations penetrate the calcium channel at different rates, with those moving through the aqueous pore at low speeds acting as competitive inhibitors of Ca^{2+} (Hurwitz, 1986). The accumulation of intracellular free Ca^{2+} can inactivate calcium channels (Hille, 1984) and also reduce calcium-dependent potassium current (Eckert and Ewald, 1982).

Several of the cations mentioned above inhibit olfactory responses (Takagi et al., 1969; Suzuki, 1978). In some cases toxic effects of multivalent cations have been observed. Industrial workers exposed to cadmium dust lose olfactory function (Arvidson, 1981). Also, degeneration of receptor cells after exposure of the olfactory epithelium to mM concentrations of $ZnSO_4$ has been observed in frogs and mammals (Adamek et al., 1984; Anholt et al., 1984).

These data support a model of olfactory transduction in which an inward calcium current may contribute to the receptor potential. The importance of cilia for olfactory transduction suggests that calcium currents could be generated along these structures. Extracted ciliary preparations from Paramecium are known to alter their orientation of beating in the presence of Ca^{2+} (Naitoh and Eckert, 1974), indicating calcium channels may be localized on cilia.

Properties of Calcium Channels

Calcium channels must be highly selective since Ca^{2+} is present in extracellular media at about 1 mM, a much lower concentration than found for other ions. Hess and Tsien (1984) proposed that calcium channel selectivity may be explained by a two-site model in which Ca^{2+} binds with higher affinity than other ions to an outer and inner site of a single-file pore. When these sites are occupied the probability of current flow is increased by the mutual repulsion of Ca^{2+}, given 1 mM extracellular Ca^{2+} . Calcium ion binding at the inner site electrostatically repulses ions with lower affinities than Ca^{2+} from the outer site, thus constituting a "selectivity filter". To illustrate, Ba^{2+} conduction through calcium channels generates larger

currents than Ca^{2+} itself (Hagiwara and Ohmori, 1982; Hille, 1984). But addition of small amounts of Ca^{2+} blocks Ba^{2+} currents because Ba^{2+} binds less strongly to the outer site (Hess and Tsien, 1984). Conversely, calcium channels can be made permeable to monovalent cations such as Na^{+} and Li^{+} by removing divalent cations (Lansman et al., 1985).

Organic calcium channel antagonists block the voltage-dependent inward flux of Ca^{2+} in a variety of tissues. It is known that organic calcium channel antagonists affect the channel gating mechanism of voltage-dependent calcium channels by slowing both calcium channel activation and recovery from previous inactivation (Glossmann et al., 1982). Garcia et al. (1986) proposed that distinct, stereospecific binding sites exist for each chemical class of organic calcium channel antagonists and together they form a complex that is functionally associated with the calcium channel. Each binding site in the complex appears to be functionally coupled to the others.

At least some organic calcium channel antagonists (i.e., 1,4-dihydropyridines) require Ca^{2+} to bind to their receptor site. Stereoselectivity of drug binding sites is present, for the (-) stereoisomer of verapamil is a more potent calcium channel antagonist than (+)-verapamil (Miller and Freedman, 1984). Verapamil binds to a site on the inner mouth of the calcium channel (Glossmann et al., 1982). Of the two diltiazem stereoisomers, the (+) isomer is the more

effective calcium channel antagonist (Garcia et al., 1986). It appears that diltiazem possesses affinity for inactivated calcium channels while verapamil has greater affinity for channels in the activated conformation (Lee and Tsien, 1983).

Types of Calcium Channels

Voltage-Dependent Calcium Channels

The most extensively studied calcium channels are those exhibiting voltage-dependent characteristics. There are several known types of voltage-dependent calcium channels which differ in drug affinity, kinetic features, and tissue specificity. These are: (1) L-type; (2) T-type; and (3) N-type.

L-type calcium channels have been observed in many cells, including cardiac and smooth muscle cells. They are voltage-dependent, producing long-lasting currents at strong depolarizations (Nowycky et al., 1985) and are affected by neurotransmitters that activate cAMP-dependent phosphorylation (Reuter, 1985). Pharmacologically, the L-type calcium channel is inhibited by 1,4-dihydropyridines (DHP's) such as nifedipine, and phenylalkylamines such as verapamil, and the benzothiazepine, diltiazem (Miller and

Freedman, 1984).

T-type calcium channels are also found in cardiac cells. They are activated at weak depolarizations and produce an inward current more transient than L-type calcium channels (Nowycky et al., 1985). T-type channels are not affected by 1,4-dihydropyridines (Reuter, 1985) nor are they sensitive to blockade by Cd^{2+} (Nowycky et al., 1985).

While the brain is one of the richest sources of high affinity binding sites for DHP calcium channel blockers (Miller and Freedman, 1984), there are calcium channels present which are insensitive to these agents, the so-called N-type channels (Reuter, 1985). Besides the presence of L- and T-type channels, N-type calcium channels are found in sensory neurons of the chick dorsal root ganglion, where they require large depolarizations for activation, and are blocked by Cd^{2+} (Nowecky et al., 1985).

Receptor-Operated Calcium Channels

Receptor-operated calcium channels (ROC's) are a separate population of calcium channels that appear to be involved in smooth muscle and secretory cell functions (Hurwitz, 1986). Receptor-operated calcium channels may be relatively insensitive to organic calcium channel antagonists (Janis and Triggle, 1984) and are not as well

characterized as voltage-dependent calcium channels. The main evidence for their existence is that agonists can stimulate Ca^{2+}-dependent contractions in a variety of tissues without altering the membrane potential (Hurwitz, 1986). In the guinea pig ileum, ROC's mediate contractions induced by activation of a variety of neurotransmitter receptors, including acetylcholine, substance P, serotonin, and histamine (Glossmann et al., 1982).

Second Messenger Systems

Cyclic Nucleotides

Recent work has strongly supported the involvement of cAMP in olfactory transduction (Lancet, 1986). Adenylate cyclase is present in isolated frog olfactory cilia with a specific activity about 15 times that of brain tissue (Pace et al., 1985). Additionally, Pace et al. (1985) report odorants enhance adenylate cyclase activity in a dose-dependent manner and require the presence of GTP.

Electrophysiological experiments suggest that cAMP has an inhibitory role in transduction. Menevse et al. (1977) found that dibutyryl cAMP (dbcAMP), a lipophilic analog of cAMP, reversibly elminates EOG's when applied to the olfactory mucosa for 1 min as a 2 mM solution. However, they

report that dibutyryl cGMP (dbcGMP), a lipophilic analog of cGMP, does not affect olfactory responses in the frog Rana temporaria. Dibutyryl cAMP is not hydrolysed by cyclic nucleotide phosphodiesterase (PDE) nor does it inhibit this enzyme (Cheung, 1970). Menevse et al. (1977) also tested a 10 mM solution of imidazole, a PDE activator. They observed a 20% increase in EOG amplitudes, presumably due to the increased hydrolysis of cAMP.

A useful compound which has not yet been applied in olfactory research is forskolin, a diterpene isolated from the roots of Coleus forskohlii, which reversibly activates adenylate cyclase in a variety of tissues without requiring a GTP-binding protein (G protein) (Seamon and Daly, 1981; Drummond, 1984). Forskolin may be quite useful in probing effects of cAMP in olfactory transduction.

Cyclic AMP may also have actions in gustatory receptor activity. Kurihara et al. (1974) reported high adenylate cyclase activity both in bovine taste buds and rabbit olfactory epithelium. Additionally, PDE occurs in higher levels in bovine taste buds than in tongue epithelial cells (Law and Henkin, 1982).

Cyclic AMP regulates many kinds of intracellular events by activating cAMP-dependent protein kinase (cAMP-PrK), which can phosphorylate numerous proteins (Cohen, 1982). Membrane ion channels are one such class of proteins that may be regulated by cAMP-PrK. In the brain, cAMP appears to

modulate potassium channel conductance in response to neurotransmitter receptor activation. In Aplysia (sea slug) neuron R15, potassium conductance is increased by serotonin (5-HT), and this response is mediated by cAMP (Adams and Levitan, 1982). Madison and Nicoll (1982) reported that both norepinephrine (NE) and cAMP block Ca^{2+}-activated K^+ conductance in rat hippocampal pyramidal cells without affecting calcium currents.

There is evidence that ion-channel proteins may be directly phosphorylated, leading to changes in their gating properties. Depayer et al. (1982) report that Ca^{2+}-activated K^+ currents in Helix (snail) neurons are enhanced after internal perfusion with the catalytic subunit (CS) of cAMP-PrK. The proposal that a regulatory component of the potassium channel is the site of phosphorylation by cAMP-PrK (Depayer et al., 1982) has been strengthened by Ewald et al. (1985) who reported that the CS changes opening and closing kinetics of individual Ca^{2+}-dependent potassium channels from Helix ganglia. The channels remain open longer after exposure to CS. Cyclic AMP-dependent protein phosphorylation may also be required for calcium channels to remain active (Rosenberg et al., 1986).

Calmodulin

Calmodulin is a ubiquitous Ca^{2+}-binding protein which participates in the regulation of Ca^{2+}-dependent processes and cAMP synthesis and degradation (Drummond, 1984). The functions of cAMP and calmodulin appear to be closely interconnected. In some cases, both cAMP and calmodulin can phosphorylate the same protein (e.g., phosphorylase kinase) (Cohen, 1982). In the presence of Ca^{2+}, the neuroleptic drug trifluoperazine (TFP) binds to calmodulin in the brain (Levin and Weiss, 1976) and prevents the calmodulin-mediated activation of PDE (Chau et al., 1982), Ca^{2+}/Mg^{2+} ATPase (Vincenzi, 1982), adenylate cyclase (Bronstrom et al., 1975), and many other enzymes (Cohen, 1982). Trifluoperazine has about five times the affinity for calmodulin as another phenothiazine, chlorpromazine (CPZ) (Levin and Weiss, 1979). Besides TFP and CPZ, other more specific calmodulin inhibitors have been developed, such as N-(6-aminohexyl)-5-chloro-1-napthalenesulfonamide (W-7) (Hidaka and Tanaka, 1982).

Inositol Phospholipids

Another second messenger system that may modulate olfactory responses is the receptor-mediated release of

diacylglycerol and inositol bis- or trisphosphate from, respectively, phosphatidylinositol 4-phosphate (PIP) or phosphatidylinositol 4,5-bisphosphate (PIP_2) by phospholipase C (Michell, 1983; Fisher et al., 1984). This enzyme appears to be the most physiologically active mechanism for polyphosphoinositide degradation in the brain (Fisher et al., 1984). A growing number of chemical messengers are being discovered to induce polyphosphoinositide turnover, acting through a wide variety of receptor types (Nishizuka, 1984).

Inositol trisphosphate (IP_3) has been proposed to mediate a rise in intracellular Ca^{2+} by release from internal stores (Fisher et al., 1984); Nishizuka, 1984). However, Glossmann et al. (1982) have reported that phospholipases A and C sharply reduce the binding of the calcium channel antagonist, nimodipine, to guinea-pig brain membranes. They postulate that membrane phospholipids may have a critical involvement in calcium channel function.

Diacylglycerol activates protein kinase C (Michell, 1983). This enzyme is associated with synaptic membranes in the brain and can phosphorylate many proteins. Tumor promoters such as 12-O-tetradecanoylphorbol 13-acetate (TPA) compete with diacylglycerol and activate protein kinase C (Michell, 1983). Phenothiazines such as chlorpromazine (CPZ) and TFP can inhibit protein kinase C, apparently by drug competition with a phospholipid cofactor, e.g.,

diacylglycerol or phosphatidylserine (Schatzman et al., 1981).

Research Rationale

There are clear indications that Ca^{2+} participates in olfactory transduction, possibly as a current carrier, a second messenger, or both. In addition, increased interest in a possible role of cAMP in olfactory transduction gives added significance to electrophysiological studies of how changes in second messenger activity affect olfactory transduction.

The roles of Ca^{2+} and cAMP in olfactory transduction were studied by quantitative application of chemical agents to olfactory mucosae by aerosol spray during extracellular recording. Inorganic cations and organic calcium channel antagonists were used to test the hypothesis that calcium channels help produce EOG's. Comparisons were made of the actions of these agents, most of which block calcium channels while others such as Ba^{2+} and Sr^{2+} can conduct current through calcium channels. Different organic calcium channel antagonists which differentiate calcium channel sub-types were tested. Second messenger roles of calmodulin and the cyclic nucleotides, cAMP and cGMP, were investigated using drugs that inhibit, mimic, or activate these systems.

CHAPTER II

METHODS

The roles of Ca^{2+} and cAMP in olfactory transduction were explored by aerosol application of inorganic cations, organic calcium channel antagonists, calmodulin antagonists, and cyclic nucleotide agonists onto the olfactory epithelium of the northern grass frog (Rana pipiens) during electrophysiological recording.

Chemical Agents

The chloride salts of certain inorganic cations block or enhance inward calcium conductance (Hagiwara and Byerly, 1983; Hille, 1984). These include La^{3+}, Cd^{2+}, Zn^{2+}, Co^{2+}, Ca^{2+}, and Mg^{2+}, all of which block calcium channels, and Sr^{2+} and Ba^{2+} which substitute for Ca^{2+} as current carriers and may enhance conductance in calcium channels. Three classes of organic calcium channel antagonists are known and include the aralkylamines (e.g., verapamil), benzothiazepines (e.g., diltiazem), and 1,4-dihydropyridines (e.g., nicardipine) (Garcia et al., 1986). Agents used in this study were verapamil, diltiazem, nicardipine, and nifedipine. However, only (+)-diltiazem and racemic

verapamil are commercially available. The anti-calmodulin agent, N-(6-aminohexyl)-5-chloro-1-naphthalenesulfonamide (W-7), was used as a probe for potential involvement of calmodulin in olfactory transduction. Chlorpromazine (CPZ) and trifluoperazine (TFP) are also calmodulin antagonists, but in addition they affect other chemical messenger signaling mechanisms. Experimental probes for cyclic nucleotide function used in this study included cAMP and cGMP themselves, their lipophilic, dibutyryl analogs (dbcAMP and dbcGMP), and an activator of cAMP synthesis (forskolin).

All drugs and reagents were obtained from Aldrich, Calbiochem, Pfalz and Bauer, or Sigma Chemical companies. Hydrophilic agents were dissolved in double distilled water and delivered as an aerosol spray. Hydrophobic agents were dissolved in dimethyl sulfoxide (DMSO) or a micro-suspension was formed using polyethylene glycol 400 (PEG 400). Dilutions to 1% solutions were made for aerosol application. Controls consisted of separate experiments with aerosol application of agents chemically similar to those being tested but with less activity (e.g., adenosine as a control for cyclic nucleotides), or aerosol application of the appropriate solvent but without the drug. All solutions were frozen between experiments and discarded after one week. All agents were stored in darkness except during aerosol application, because many are known to be light-sensitive (e.g., the 1,4-dihydropyridines).

Surgery and Anesthesia

Frogs were anesthetized and immobilized with subcutaneous injections of 250 mg/kg urethane and 15 mg/kg d-tubocurarine chloride into the dorsal lymph sac. The ventral olfactory mucosa was surgically exposed by removal of the external nares with the associated integument, skull material, and dorsal olfactory mucosa (Figure 1).

Odorant Stimulation

A standard odorant stimulating and recording system was used (Schafer et al., 1984; Figure 1). Clean air supplied by an air compressor was passed through activated charcoal, humidified, then delivered to the olfactory mucosa at a delivery rate of 850 ml/min through 0.75 cm i.d. orifices situated 4.3 cm from the mucosa. The odorant reservoirs in the stimulating system (Figure 1) contained sufficient odorant in liquid form (0.3-1.5 ml dispersed on a 5 cm diameter disk of filter paper) to saturate a 1,000 ml air volume for many hours of constant stimulation. The standard odorant, isoamyl acetate (IAA), was delivered as a saturated vapor in air to the surgically-exposed ventral olfactory mucosae every 100 sec in 0.3 sec pulses. Other odorants, including cyclohexanol, cyclopentanone, cyclopentanol, and

dimethyl disulfide were used periodically to verify that the effects observed with IAA were representative of the effects on responses to other odorants.

Automatic odorant stimulation was programmed using a master pulse generator (WPI series 800 system) which drove a Grass S88 stimulator connected to low current relays which actuated the system of electric valves in the olfactometer (Figure 1). Aerosol stimuli were initiated manually through a separate channel driven by the Grass stimulator with a separate solenoid valve system.

Electrophysiological Recording

Extracellular stimulating and recording methodology described by Schafer et al. (1984) was used to record the slow, surface-negative potential (electroolfactogram, or EOG) elicited from olfactory receptor neurons in the ventral olfactory epithelium. A Ringer/agar-filled capillary electrode with a tip diameter of approximately 100 μm was placed onto the crest of the olfactory eminence, a mound-like landmark at the approximate center of the mucosa. Electroolfactogram responses were amplified by a Tektronix 5A22N differential amplifier. Waveforms were displayed in DC mode on a Tektronix D11 analog storage oscilloscope or a 5223 digitizing oscilloscope, and the AC waveform amplitude

recorded continuously with a Soltec 1242 chart recorder.

Aerosol Application of Agents

An aerosol delivery system developed in this laboratory was used to apply aqueous solutions onto the epithelial surface. Aerosol drug delivery to the olfactory mucosa is preferable to irrigation techniques such as lavage, because application of fluids on the mucosa disrupts electrophysiological recording (Schafer et al., 1986). The aerosol delivery system consisted of a DeVilbiss no. 40 glass nebulizer connected through ground glass fittings to a 0.75 cm i.d. orifice situated 4.3 cm from the mucosa. Aerosols were produced from nitrogen gas with an output flowrate adjusted to 10 l/min. Control tests with the nebulizer unloaded produced only small, positive-going waves. This nebulizer produces small aerosol droplets with a median diameter of 1-10 μm (Hinds, 1982). The surface distribution of aerosol droplets was assessed for uniformity by scanning electron microscopy (Figure 2a and 2b).

Calibration of Aerosol Delivery Rate

The aerosol delivery rate was calibrated by three different methods:

1. Calibration by Acid-Base Titration

A 7 mm diameter filter paper disk (38.5 mm^2) saturated with 6 µl of 0.1 M HCl was supported on a plastic film placed on the frog's external naris. The nebulizer was loaded with a solution of 0.9 M Na_2CO_3 and 0.001 M phenolphthalein indicator. The aerosol was sprayed onto the mucosa in 1 sec increments, allowing a few seconds between each application to permit the mixture to react. The average cumulative time required for a permanent color change was 7 sec.

Since the filter paper disk holds 6.0×10^{-7} mol HCl, the volume of base required to neutralize the acid is 6.0×10^{-7} mol/0.9 M Na_2CO_3 = 6.67×10^{-7} l or 0.667 µl. The aerosol delivery rate (R) is expressed as:

$$R = 0.667\ \mu l/(38.5\ mm^2 \times 7\ sec) = 2.5 \times 10^{-3}\ \mu l/mm^2\text{-sec.} \quad [1]$$

With an average olfactory mucosa surface area (A) of 5.9 mm^2 (N=6; SD=0.07) the rate of aerosol delivery to the entire

olfactory mucosa is R X A = 0.015 µl/sec.

2. Calibration by Aerosol Weight

Aerosol sprays of water were collected in a vial with an opening the size of the frog olfactory mucosa situated 4.3 cm from the aerosol delivery orifice. The water collected after several minutes of delivery time was weighed on a Mettler AE 100 digital balance. The value for R was calculated at 3.6×10^{-3} µl/mm^2-sec.

3. Calibration by High Performance Liquid Chromatography

Aerosol sprays of 1 M phenol were collected as in the above method, except the delivery time was shortened and the vial contained 1 ml water to help capture and dilute the phenol. The sample and known standards were run on a Vydac reverse phase column (no. 201TP54) with a Gilson model 302 pump and the gradient run by an Apple IIe computer. A value for R of 2.0×10^{-3} µl/mm^2-sec was determined by measuring peak areas. Pooling data from all three calibration techniques gives an average delivery rate of:
R = 2.7×10^{-3} µl/mm^2-sec.

Calculation of Agent Concentration on the Olfactory Mucosa

Given a mucous layer thickness of 0.03 mm (Getchell, 1980) the mucous volume (V_m) on the olfactory mucosa is:

$$V_m = 0.03 \text{ mm} \times A = 0.177 \text{ mm}^3 \text{ or } 0.177 \ \mu l. \qquad [2]$$

Since the product of molarity and volume is moles, the number of moles delivered to the olfactory mucosa per sec can be expressed as ($C_n TRA$), where (C_n) represents the solute concentration in the nebulizer and (T) represents delivery time in sec. The delivered moles are divided by the new mucous volume (which has increased after aerosol delivery) to give the calculated final concentration of solute (C_f):

$$C_f = (C_n TRA)/(V_m + TRA) \qquad [3]$$

Equation 3 may be simplified to

$$C_f = C_n/[1 + (V_m/TRA)]. \qquad [4]$$

Substituting the above values into Eq. 4 with $C_n = 10^{-4}$M, a value of 1.5×10^{-5}M is obtained for C_f, which is almost one order of magnitude lower than C_n. Since C_n was usually 10^{-3}M or 10^{-4}M, most of the values reported for C_f were

1.5 X 10^{-4}M or 1.5 X 10^{-5}M, respectively.

Most solutions loaded into the nebulizer had solute concentrations in the millimolar range. The actual final concentration of solute after delivery to the olfactory mucosa was probably less than the calculated value, because of dilution by the mucous flow produced by the olfactory epithelium. The rate of mucous secretion could not be measured and is not incorporated in the calculations. Qualitative observations of the rate of dye movement in the mucus suggested a copious secretion. The mucous flow is driven by cilia to a rapid drainage through the internal naris.

Normalization of Data and Analysis

Preparations which gave an initial baseline EOG magnitude of less than 1 mV were rejected to reduce the possibility of variability in the data introduced by using less-than-healthy mucosae. The pre-treatment baseline was taken as the mean amplitude of the last five EOG's prior to application of an agent. The course and extent of changes in the mV amplitude of EOG's following agent delivery were monitored over 33 min, post-treatment (20 EOG's). The 20 post-treatment EOG's were expressed as a percentage of the baseline and averaged from four or more trials to determine

the percent inhibition produced by a given agent at a given concentration. While averaging together many EOG's decreases the measurement sensitivity, the resulting statistical data has greater reliability.

Electroolfactogram data were then analyzed by: (1) rank ordering, as in the case of inorganic ions; (2) comparisons of inhibition or enhancement by agents with known differences in activity or ability to penetrate the membrane (e.g., cAMP and dbcAMP); and (3) statistical analyses (i.e., one-way analysis of variance for fixed effects).

In many cases, complete recovery to baseline was observed following agent application, allowing further experiments to be performed on the same mucosa. These additional experiments involved different agents to insure that no data set was biased by multiple samples of the effects of the same agent on the same tissue. The exception for this protocol was the use of dilution series to construct dose-response curves. An estimate of the concentration of agent producing half-maximal inhibition (IC_{50}) was made from the curves fitted to dilution series data. In this case, multiple tests of the same agent were performed on the same olfactory mucosa with lower concentrations preceding higher ones.

Are Post-Treatment Effects Correlated with Baselines?

Tests for correlations between post-treatment EOG inhibition and pre-treatment baselines are useful to prevent artifacts of data analysis by the use of percentages alone. For example, a positive correlation might give false indications of inhibition if many of the experiments had high pre-treatment baselines.

A test of the null hypothesis (i.e., the true correlation is zero) was made with a t test described by Hays (1981) to determine whether post-treatment EOG amplitudes were linearly correlated either negatively or positively with pre-treatment baselines. The values of t were determined from ten sets of experiments with N of not less than four for each set. As shown in Table I, in no case did t exceed the value necessary to reject the null hypothesis in a two-tailed test. Figure 3 shows a scattergram of pre-treatment baseline amplitudes plotted against percent inhibition for experiments with a calculated final concentration of 1.5×10^{-5}M diltiazem, verapamil, and forskolin. There is no significant statistical correlation of EOG inhibition with the pre-treatment baseline amplitude. Normally, multiple t tests are inappropriate since they lead to an increased probability of obtaining significant results by chance. But t was never found to be significant, which supports the validity of the null hypothesis.

TABLE I

REGRESSION STATISTICS ON INHIBITION AND BASELINE DATA

Agent	Final Concentration	Correlation Coefficient*	T Ratio**	DF
Adenosine	1.5×10^{-4}M	0.771	1.713	2
cAMP	1.5×10^{-4}M	0.034	0.005	2
cGMP	1.5×10^{-4}M	0.087	-0.151	3
CPZ	1.5×10^{-4}M	0.729	1.504	2
dbcAMP	1.5×10^{-4}M	-0.660	-1.260	2
Diltiazem	1.5×10^{-5}M	-0.163	-0.331	4
Forskolin	1.5×10^{-5}M	-0.397	-0.866	4
Nicardipine	1.5×10^{-5}M	0.021	0.030	2
Verapamil	1.5×10^{-5}M	-0.698	-1.950	4
W-7	1.5×10^{-4}M	0.200	0.288	2

*The correlation coefficient describes the degree and direction of a relationship between the pre-treatment baseline and EOG inhibition. Values approaching zero indicate a lack of relationship while values of one or negative one describe a perfect relationship.

**To reject the null hypothesis in a two-tailed test, $t>4.303$ (df=2); $t>3.182$ (df=3); $t>2.776$ (df=4) (Hays, 1981). Therefore the null hypothesis of no correlation between EOG inhibition and pre-treatment baseline amplitude is accepted. Since no correlation exists, EOG inhibition data is not biased from experiments with unusually high or low pre-treatment baselines.

Figure 1.

System used for odorant and aerosol delivery and for electrophysiological recording.

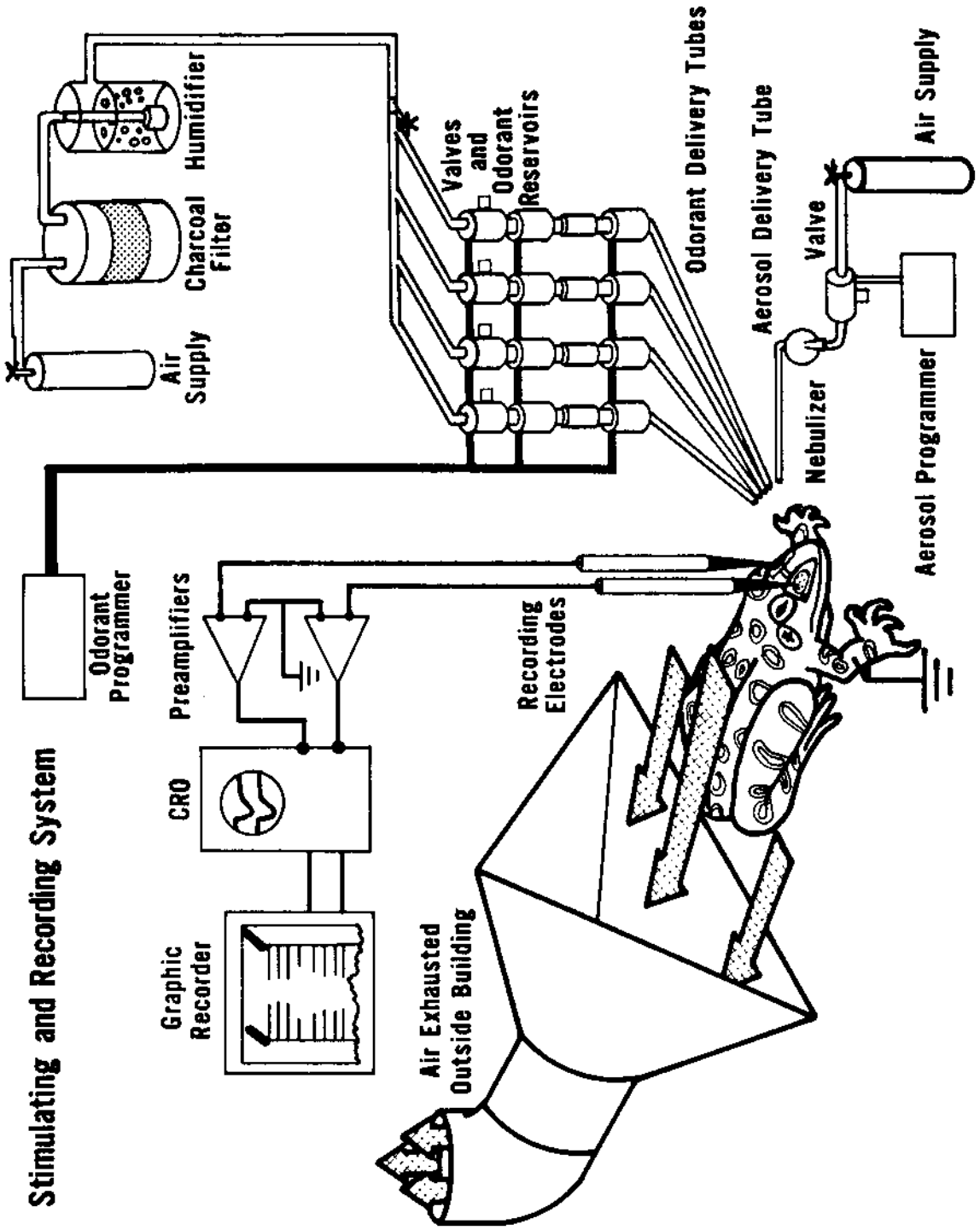
Stimulating and Recording System
Odorant Programmer
Preamplifiers
CRO
Graphic Recorder
Recording Electrodes
Air Exhausted Outside Building
Aerosol Programmer
Nebulizer
Aerosol Delivery Tube
Valve
Air Supply
Odorant Delivery Tubes
Valves and Odorant Reservoirs
Humidifier
Charcoal Filter
Air Supply

Figure 2a.

Scanning electron micrograph of aerosol dispersion pattern from 0.25 sec delivery of 0.5 M $BaCl_2$ onto a gold-coated cover glass (X 50). Aerosol application took place under standard stimulating conditions. Barium chloride deposits completely cover the surface (2.3mm X 3.3mm), which is of comparable size to the frog ventral olfactory mucosa.

Figure 2b.

Pattern of $BaCl_2$ deposits (X 200) at periphery of the same aerosol dispersion pattern shown in Figure 2a.

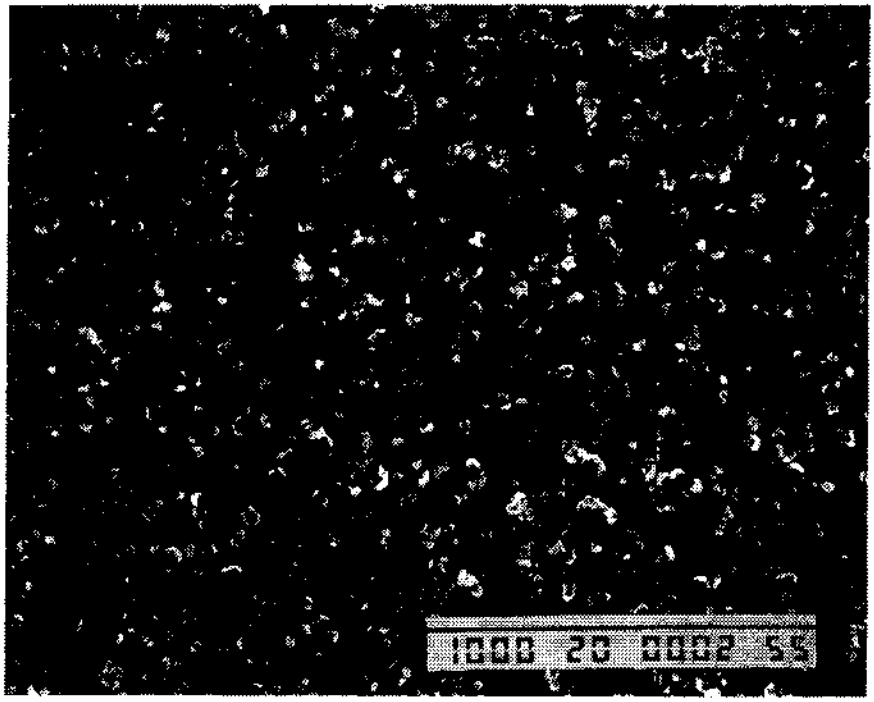

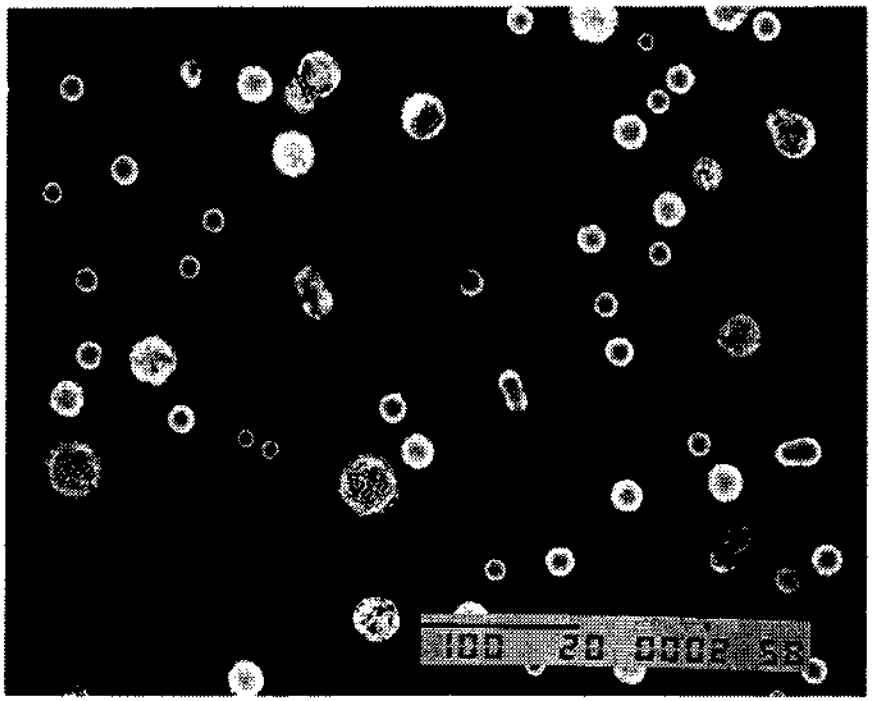

Figure 3.

Scattergram of pre-treatment baseline EOG amplitudes (DC mV) plotted against percent inhibition of EOG responses. Diltiazem (N = 6, squares), forskolin (N = 6, triangles), and verapamil (N = 6, circles) were applied to give a calculated final concentration of 1.5×10^{-5}M.

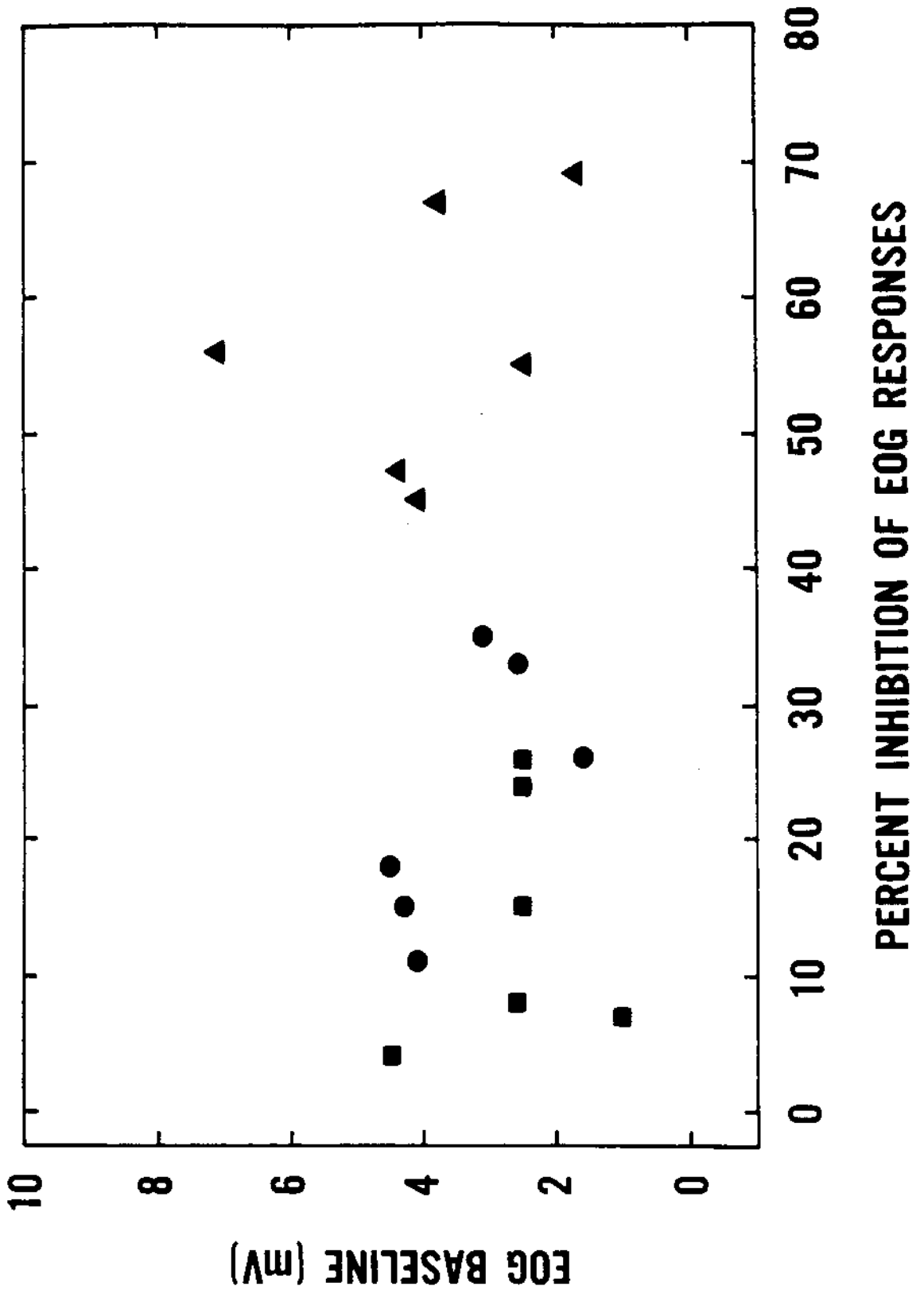
EOG BASELINE (mV)
10
8
6
4
2
0
0
10
20
30
40
50
60
70
80
PERCENT INHIBITION OF EOG RESPONSES

CHAPTER III

RESULTS

Solvents for Drug Delivery

Aerosol experiments with delivery solvents alone were used to generate control recovery curves (Figure 4). In separate experiments, aerosol application of distilled water, 1% DMSO, and 1% PEG 400 each produced low to moderate levels of inhibition when averaged over 20 post-treatment EOG's. Water inhibits EOG's by 5% (N = 10), while 1% DMSO (a 143 mM solution) inhibits by 19% (N = 7). One percent PEG 400 (a 28.15 mM solution) exhibits an unusual recovery curve (Figure 4) in which EOG's are enhanced initially after aerosol application. An initial enhancement of about 20% (N = 6) is masked by subsequent inhibition when all 20 post-treatment EOG's are averaged, giving a net inhibition of about 4% (N = 6). While PEG 400 might seem preferable to DMSO because it is less inhibitory, DMSO is less viscous and is a better solvent for extremely hydrophobic compounds such as the 1,4-dihydropyridines. The bimodal effect of 1% PEG 400 on EOG amplitudes (first enhancing, then inhibiting post-treatment EOG's) also introduces complexities in data interpretation that can be avoided by using 1% DMSO.

Ethanol is sometimes used to dissolve hydrophobic compounds, but is inappropriate for use with calcium channel antagonists since at pharmacologically relevant concentrations, ethanol blocks voltage-dependent calcium channels (Leslie et al., 1983; Leslie et al., 1986). To compare the actions of ethanol with DMSO and PEG 400, 0.1 M solutions of each solvent were tested for enhancement or inhibition (Figure 5). At a calculated final concentration of 0.015 M, all three solvents inhibited EOG's. Ethanol inhibited EOG's by 25% (N = 4), while DMSO inhibited by 16% (N = 5), and PEG 400 inhibits by 18% (N = 4).

Inorganic Ions Which Affect Calcium Channel Conductance Modify EOG Responses

Inorganic divalent and trivalent cations which block calcium channels in other tissues inhibited EOG responses by varing degrees, ranging from no effect to complete inhibition. Aerosol sprays of 2 sec duration were applied to give a calculated final concentration of 7.5 mM. Figure 6 illustrates EOG inhibition of 13% by Co^{2+} (N = 6), 23% by Ca^{2+} (N = 4), and 25% by Sr^{2+} (N = 5). Figure 7 illustrates inhibition of 33% by Al^{3+} (N = 5), 61% by Cd^{2+} (N = 6), and 61% by Zn^{2+} (N = 5). The inhibition from each of these cations is partial and reversible at this concentration,

except for La^{3+}, which virtually eliminates EOG's with no recovery over the 33 min post-treatment period (Figure 7). Slight recovery was observed from La^{3+} inhibition in experiments lasting an hour or more. Magnesium ion produces no measurable inhibition or enhancement (N = 5). As shown in Figure 7, Ba^{2+} significantly enhances EOG's by as much as 30% for the first two post-treatment EOG's ($F=43.04$; $p<0.001$, $df=19$), then produces moderate inhibition with recovery to the baseline. Averaging the 20 post-treatment EOG's after Ba^{2+} application gives 6% inhibition (N = 5).

As Shown in Figure 8, the rank order of potency of the inorganic cations in inhibiting EOG's is:

$$(La^{3+}) > (Zn^{2+}, Cd^{2+}) > (Al^{3+}, Ca^{2+}, Sr^{2+}) > (Co^{2+}).$$

Table II compares the rank order of EOG-inhibiting potency with several rankings of their effectiveness as calcium channel antagonists in other tissues. A composite rank order derived from several rankings of calcium channel blocking ability enabled statistical testing for a correlation with the EOG-inhibitory ranking. The composite rank order is:

$$(La^{3+})>(Cd^{2+})>(Zn^{2+})>(Co^{2+})>(Ba^{2+})>(Ca^{2+})>(Sr^{2+}, Mg^{2+}).$$

A significant correlation exists between the composite rank order for calcium channel blockade in other tissues and the

rank order of EOG inhibition in these experiments (R=79%; t=3.189; p<0.01; df=6). This supports the hypothesis that calcium channels contribute to EOG production, perhaps by their calcium currents.

In a dose-response curve constructed for EOG inhibition by Ca^{2+} (Figure 9), the concentration of agent producing half-maximal inhibition (IC_{50}) is estimated to be approximately 60 mM. The lowest calculated final concentration of Ca^{2+} tested, 1.5 X 10^{-4}M, significantly inhibits EOG's beyond water controls (F=5.74; p=0.0355; df=12).

Certain Organic Calcium Channel Antagonists are Inhibitory

The organic calcium channel blockers d-cis-diltiazem (hereafter referred to as diltiazem), (+/-)-verapamil (racemic verapamil; hereafter referred to as verapamil), nicardipine, and nifedipine were tested for inhibitory effects. Diltiazem and verapamil both inhibited EOG's at a calculated final concentration of 1.5 X 10^{-4}M (Figure 10). Diltiazem was less inhibitory than verapamil (Figure 11), giving 17% inhibition (N = 4), while verapamil inhibited by 36% (N = 5). Dose-response curves constructed from experiments with dilution series of diltiazem and verapamil

indicate that diltiazem had less intrinsic activity than verapamil, producing 34% inhibition (N = 5) at the highest calculated final concentration tested of 1.5 X 10^{-3}M (Figure 12), while verapamil inhibited by 54% (N = 5) at this concentration (Figure 13). The IC_{50} for verapamil is approximately 7.9 X 10^{-4}M (Figure 13). Verapamil produced significant inhibition compared to water control experiments at a calculated final concentration as low as 1.5 X 10^{-5}M ($F=26.03$; $p=0.0003$; $df=12$).

Neither of the two 1,4-dihydropyridines tested, nicardipine nor nifedipine, inhibited any more than 1% DMSO controls at a calculated final concentration of 1.5 X 10^{-5}M (Figures 14 and 15). The extremely hydrophobic nature of nicardipine and nifedipine prevented experiments at higher drug concentrations in 1% DMSO solutions.

Actions of Calmodulin Antagonists

The calmodulin antagonists trifluoperazine (TFP), chloropromazine (CPZ), and N-(6-aminohexyl)-5-chloro-1-naphthalenesulfonamide (W-7) inhibited EOG responses. W-7, the most potent (Hidaka and Tanaka, 1982), inhibited the first post-treatment EOG up to 80% in comparison with the 1% PEG 400 control curve. However, the W-7 curve and the 1% PEG 400 control curve merged rapidly (Figure 16). Both CPZ

and TFP were less inhibitory than W-7 immediately following aerosol application, but exerted longer-lasting inhibition (Figure 17). When averaged over 20 post-treatment EOG's, W-7 inhibited by 27% (N = 7), CPZ by 31% (N = 4) and TFP by 23% (N = 4).

Evidence for Involvement of cAMP in Olfactory Transduction

The cyclic nucleotides cAMP and cGMP and their lipophilic analogs, dibutyryl cAMP (dbcAMP) and dibutyryl cGMP (dbcGMP) were tested for inhibition or enhancement of EOG's. Adenosine was included as a control and to test the possible involvement of adenosine receptors in olfactory transduction. Dibutyryl cAMP was most inhibitory by far (Figures 19 and 20). At a calculated final concentration of 1.5×10^{-4}M, dbcAMP inhibited EOG's by 54% (N = 4) while dbcGMP inhibited by 20% (N = 4). Cyclic AMP inhibited by 13% (N = 4) and cGMP inhibited by 10% (N = 6). Adenosine was least inhibitory, reducing EOG's by 7% (N = 4).

Forskolin, a reversible activator of adenylate cyclase (Seamon and Daly, 1981), inhibited EOG's by 57% (N = 6) at a calculated final concentration of 1.5×10^{-5}M. The recovery curve in figure 21 shows that EOG inhibition by forskolin is reversible. A dose-response curve for forskolin (Figure 22), gives an IC_{50} of approximately 1.5×10^{-5}M.

Rank Order of Organic Agents by EOG Inhibitory Potency

Table III includes the percent EOG inhibition produced by all organic agents at a final calculated concentration of 1.5×10^{-4}M, except for nicardipine and nifedipine which were tested at a final calculated concentration of 1.5×10^{-5}M (one-tenth that of the others). At these concentrations, the organic agents can be rank ordered for EOG inhibitory potency:

Forskolin>>dbcAMP>(Verapamil,CPZ)>(W-7,TFP)>Diltiazem.

TABLE II

COMPARISON OF RANK ORDER FOR EOG INHIBITION WITH RANK ORDER FOR CALCIUM CHANNEL BLOCKADE

Ion	A	B	C	D	E	F
La^{3+}	1	1	2	1	1	1
Cd^{2+}	3	2	1	-	2	2
Zn^{2+}	2	2	-	2	-	3
Co^{2+}	6	2	4	2	3	4
Ni^{2+}	-	-	3	4	4	-
Al^{3+}	4	-	-	-	-	-
Mn^{2+}	-	4	4	3	5	-
Ba^{2+}	7	3	5	-	-	5
Ca^{2+}	5	5	6	5	-	6
Sr^{2+}	5	6	-	6	-	7
Mg^{2+}	7	7	5	6	6	7

A. Rank order of EOG inhibitory effectiveness.

B. Rank order of Ca^{2+}-activated potassium channel blocking effectiveness in human T lymphocytes (DeCoursey et al., 1984a).

C. Rank order of inhibitory effectiveness against [^{3}H]nitrendipine binding to homogenized rat cortex (Ehlert et al., 1982).

D. Rank order of calcium channel blocking effectiveness in barnacle muscle fiber (Hagiwara and Takahashi, 1967).

E. General rank order of calcium channel blocking effectiveness (Hagiwara and Byerly, 1983).

F. Composite rank order of calcium channel blocking effectiveness, derived from rank orders B, C, D, and E.

TABLE III

EFFECTS OF PROBES ON EOG RESPONSES

Agent	N	Final Concentration	Percent Inhibition
SOLVENTS			
DMSO	5	1.5 X 10^{-2}M	16 +/- 9
Ethanol	4	"	25 +/- 9
PEG 400	4	"	18 +/- 5
INORGANIC SALTS			
$AlCl_3$	5	7.5 X 10^{-3}M	33 +/- 8
$BaCl_2$	5	"	6 +/- 12
$CaCl_2$	5	"	23 +/- 5
$CdCl_2$	6	"	61 +/- 11
$CoCl_2$	6	"	13 +/- 3
$LaCl_3$	4	"	97 +/- 1
$MgCl_2$	5	"	00 +/- 3
$SrCl_2$	5	"	25 +/- 8
$ZnCl_2$	5	"	74 +/- 7
CALCIUM CHANNEL ANTAGONISTS			
Diltiazem	4	1.5 X 10^{-4}M	17 +/- 5
Verapamil	5	"	36 +/- 4
Nicardipine	4	1.5 X 10^{-5}M	18 +/- 9
Nifedipine	4	"	26 +/- 10
CALMODULIN ANTAGONISTS			
CPZ	4	1.5 X 10^{-4}M	31 +/- 6
TFP	4	"	23 +/- 11
W-7	7	"	27 +/- 7
CYCLIC NUCLEOTIDES AND MIMICS			
Adenosine	4	1.5 X 10^{-4}M	7 +/- 4
cAMP	4	"	13 +/- 7
cGMP	6	"	10 +/- 7
Dibutyryl cAMP	4	"	54 +/- 15
Dibutyryl cGMP	4	"	20 +/- 4
ADENYLATE CYCLASE ACTIVATOR			
Forskolin	4	1.5 X 10^{-4}M	93 +/- 6

Figure 4.

Averaged recovery curves following 2 sec aerosol sprays of distilled water (N = 9); 1% DMSO (N = 7); and 1% PEG 400 (N = 6).

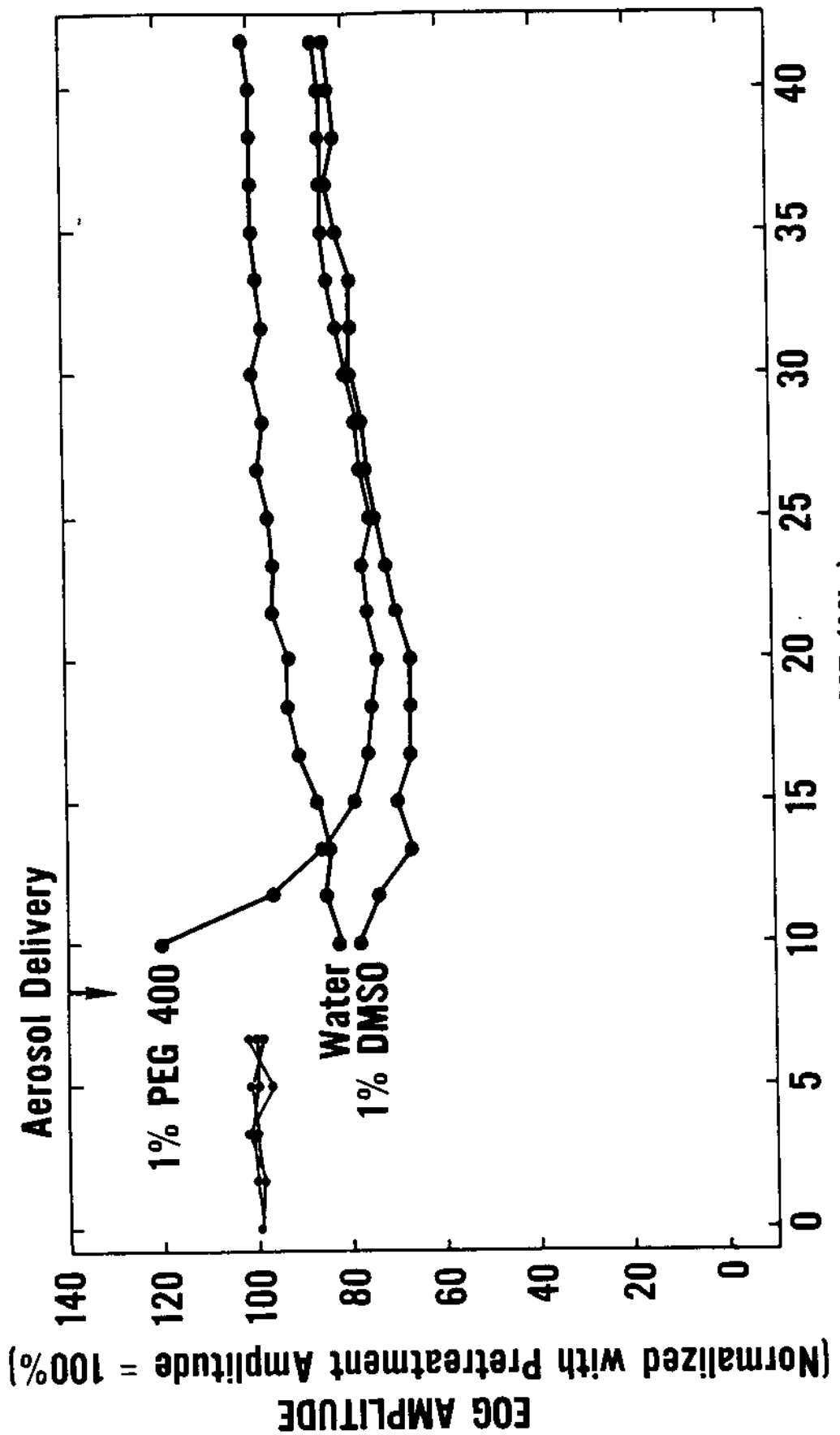
EOG AMPLITUDE
(Normalized with Pretreatment Amplitude = 100%)
140
120
100
80
60
40
20
0
0
5
10
15
20
25
30
35
40
TIME (Min)
Aerosol Delivery
1% PEG 400
Water
1% DMSO

Figure 5.

Bar graph of percent inhibition averaged over 33 min post-treatment. Dimethyl sulfoxide, ethanol, and PEG 400 were applied to give a calculated final concentration of 0.015 M. Results are means +/- SD for the number of trials given in parentheses.

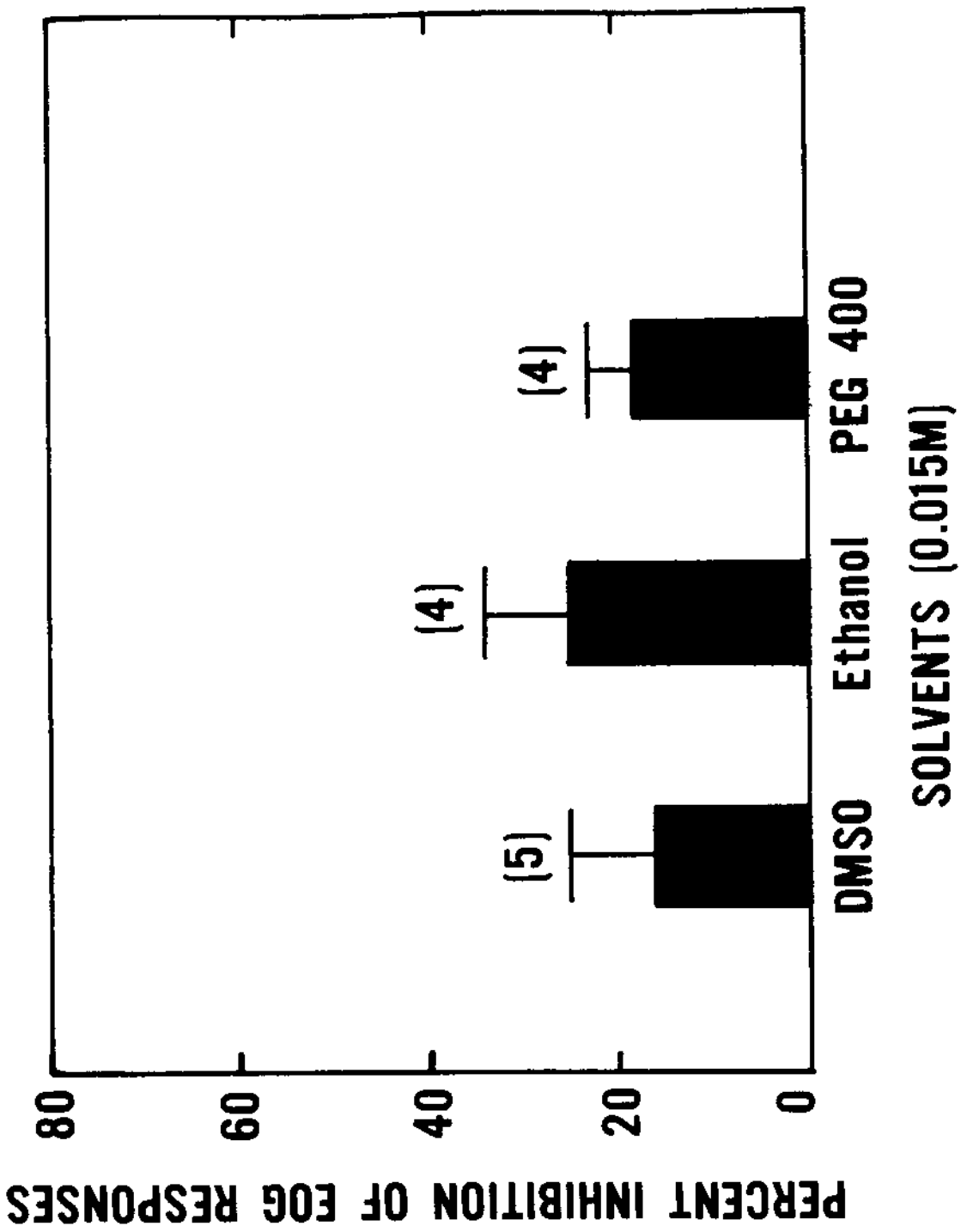
PERCENT INHIBITION OF EOG RESPONSES
0
20
40
60
80
(5)
(4)
(4)
DMSO
Ethanol
PEG 400
SOLVENTS (0.015M)

Figure 6.

Averaged recovery curves following 2 sec aerosol sprays of the chloride salts of Mg^{2+} (N = 5), Co^{2+} (N = 6), Sr^{2+} (N = 5), and Ca^{2+} (N = 5). All were applied to give a calculated final concentration of 7.5 X 10^{-3}M. Bars represent SD.

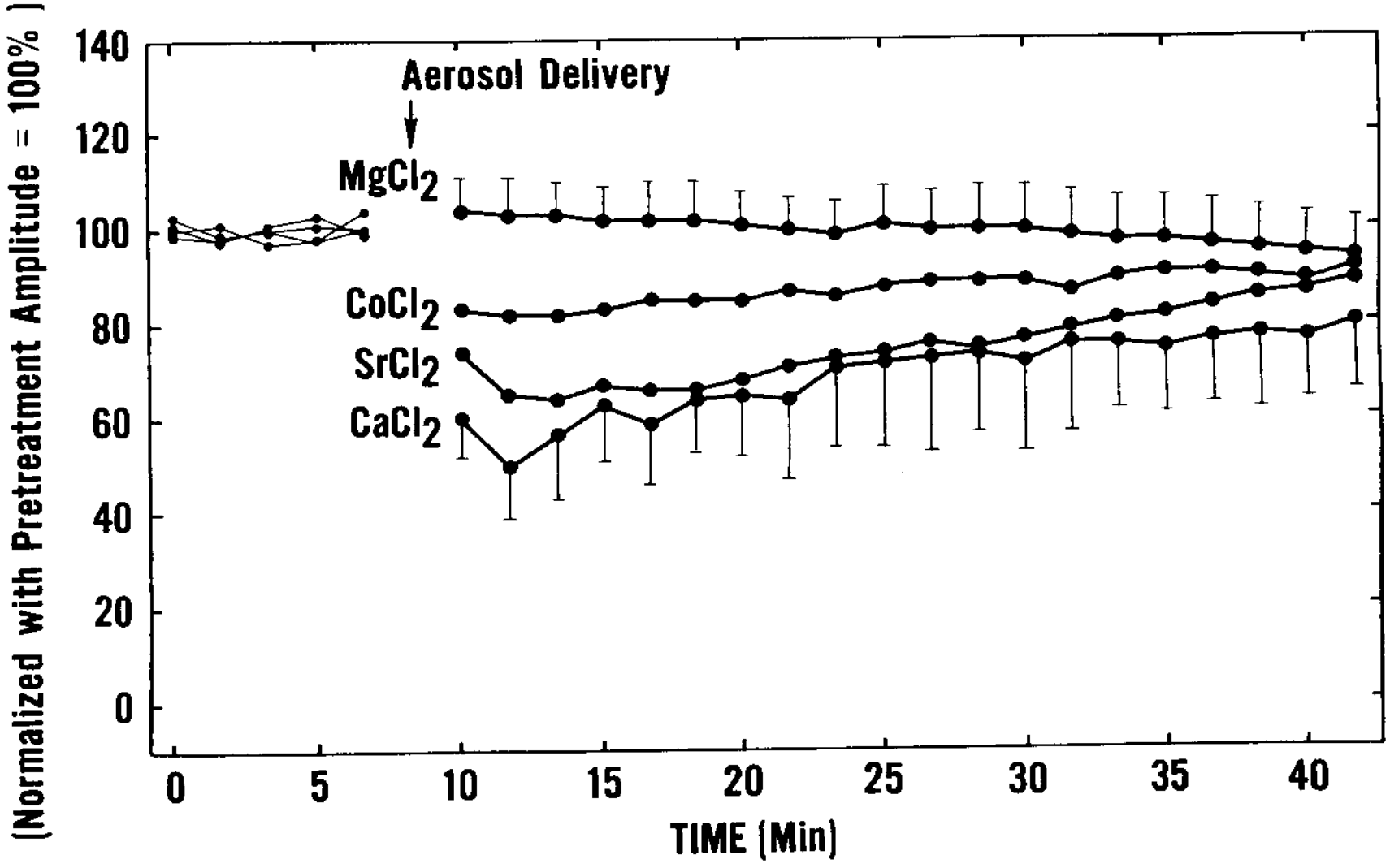
EOG AMPLITUDE
(Normalized with Pretreatment Amplitude = 100%)
140
120
100
80
60
40
20
0
Aerosol Delivery
MgCl2
CoCl2
SrCl2
CaCl2
0
5
10
15
20
25
30
35
40
TIME (Min)

Figure 7.

Averaged recovery curves following 2 sec aerosol sprays of the chloride salts of Ba^{2+} (N = 7), Al^{3+} (N = 5), Zn^{2+} (N = 5), Cd^{2+} (N = 6), and La^{3+} (N = 5). All were applied to give a calculated final concentration of 7.5×10^{-3}M. Bars represent SD.

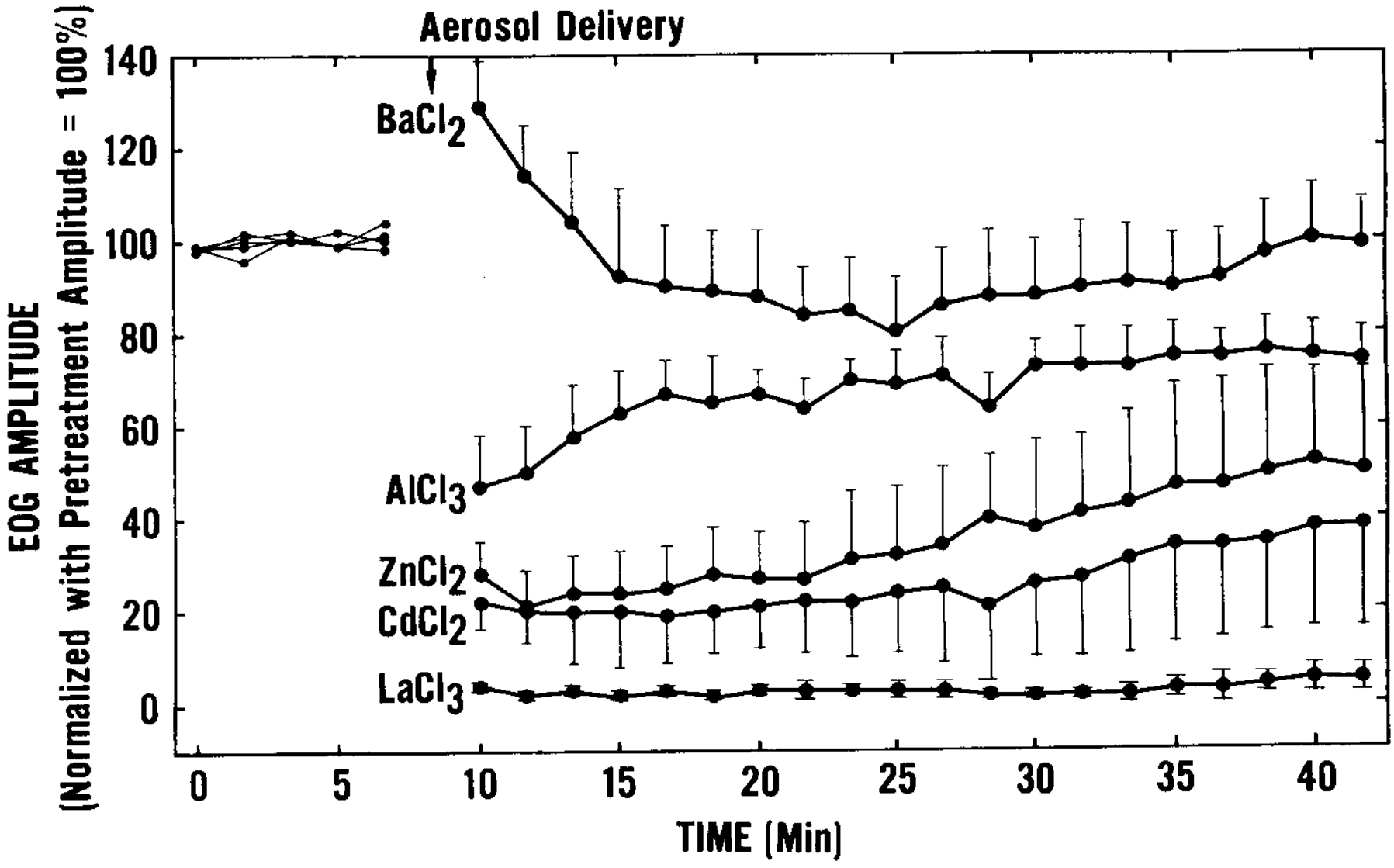
Aerosol Delivery
EOG AMPLITUDE
(Normalized with Pretreatment Amplitude = 100%)
140
120
100
80
60
40
20
0
BaCl2
AlCl3
ZnCl2
CdCl2
LaCl3
0
5
10
15
20
25
30
35
40
TIME (Min)

Figure 8.

Bar graph of percent inhibition averaged over 33 min post-treatment. The chloride salts of multivalent cations were applied to give a calculated final concentration of 7.5×10^{-3} M. Results are means +/- SD for the number of trials given in parentheses.

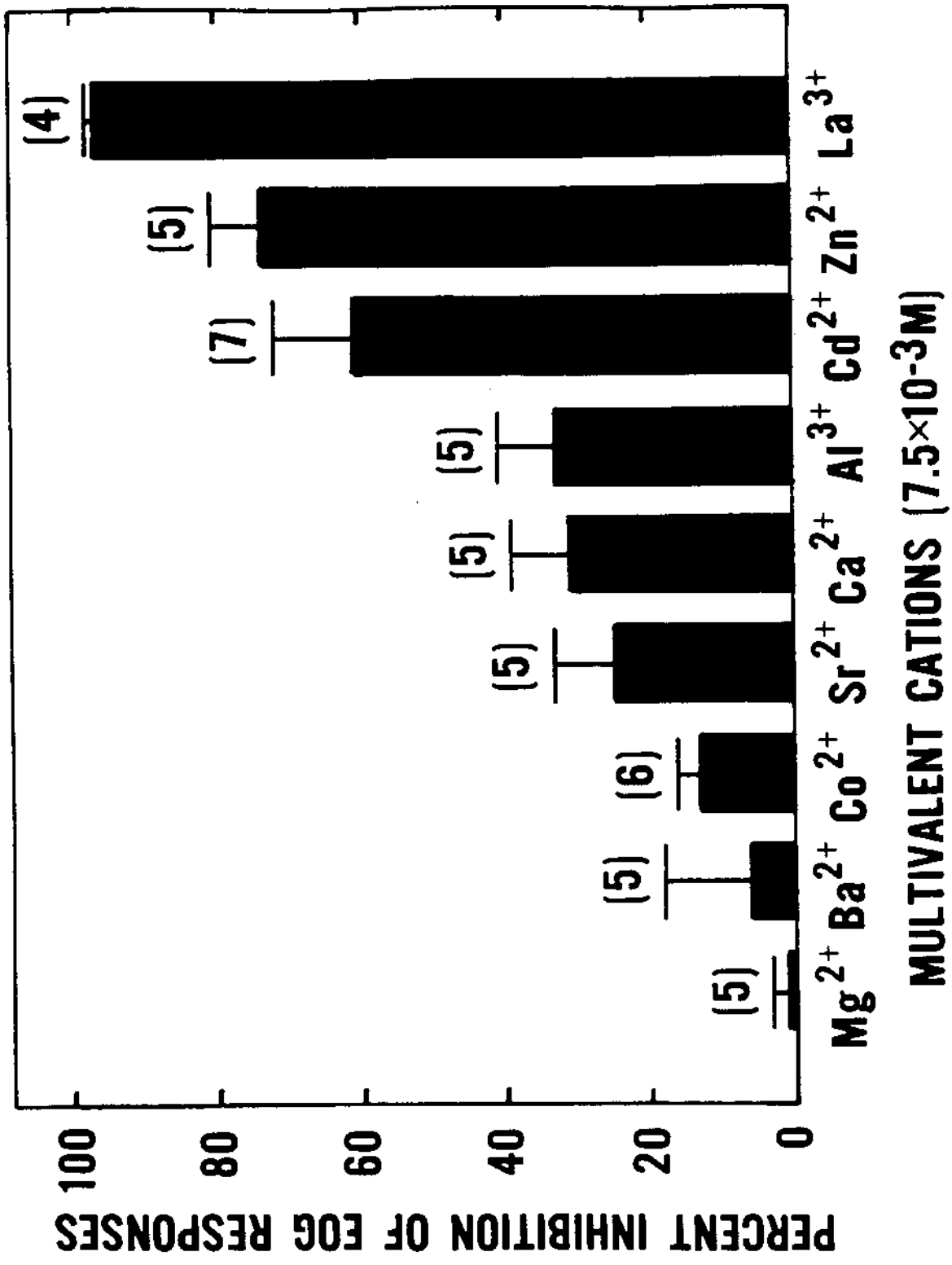
PERCENT INHIBITION OF EOG RESPONSES
0
20
40
60
80
100
(5)
(5)
(6)
(5)
(5)
(5)
(7)
(5)
(4)
Mg^{2+} Ba^{2+} Co^{2+} Sr^{2+} Ca^{2+} Al^{3+} Cd^{2+} Zn^{2+} La^{3+}
MULTIVALENT CATIONS (7.5×10-3M)

Figure 9.

Dose-response curve for Ca^{2+}. Each point represents the mean +/- SD from four or more experiments.

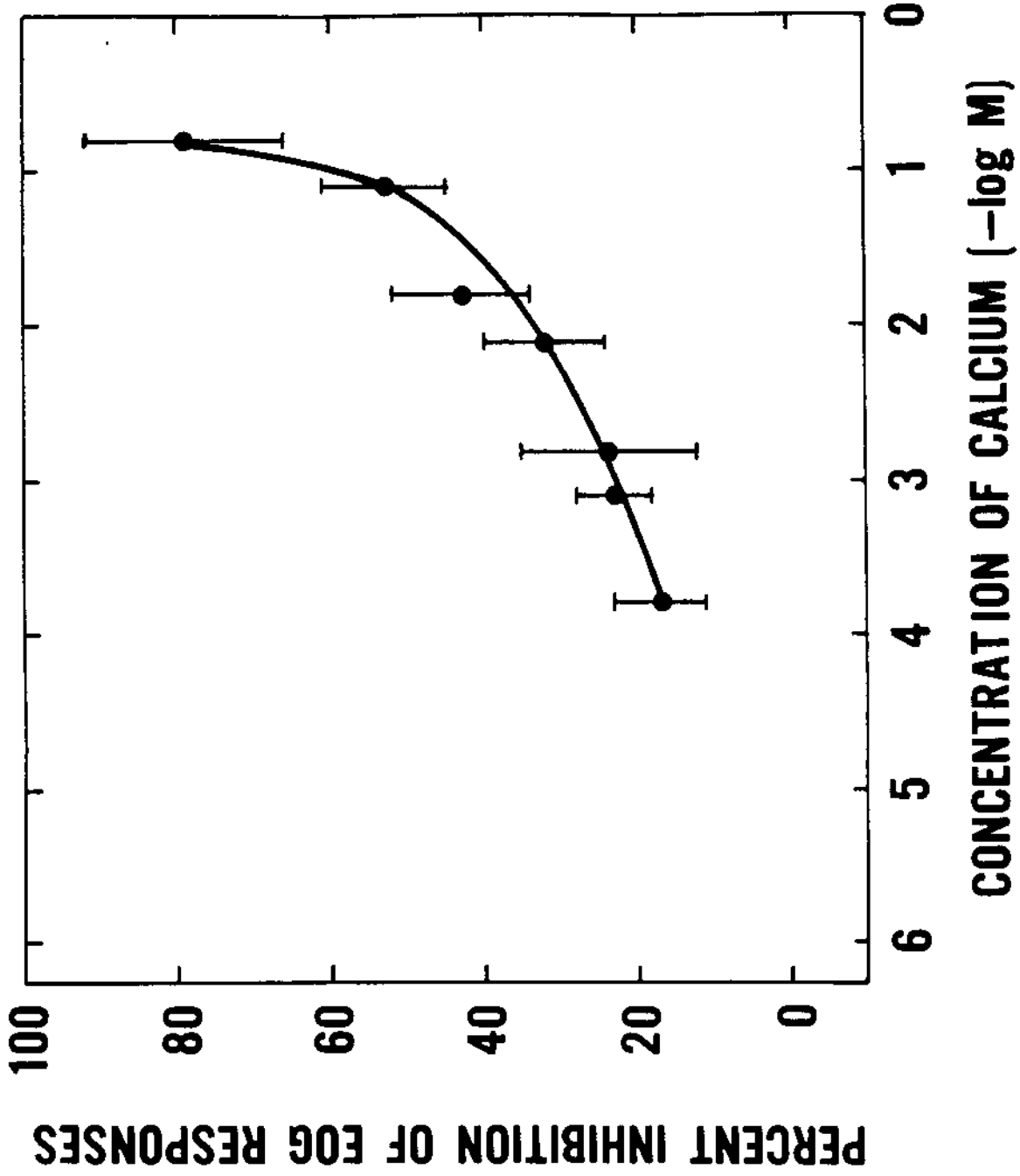
PERCENT INHIBITION OF EOG RESPONSES
100
80
60
40
20
0
6
5
4
3
2
1
0
CONCENTRATION OF CALCIUM (−log M)

Figure 10.

Averaged recovery curves following 2 sec aerosol sprays of diltiazem (N = 7) and verapamil (N = 8). Both were applied to give a calculated final concentration of 1.5 X 10^{-5}M. Bars represent SD.

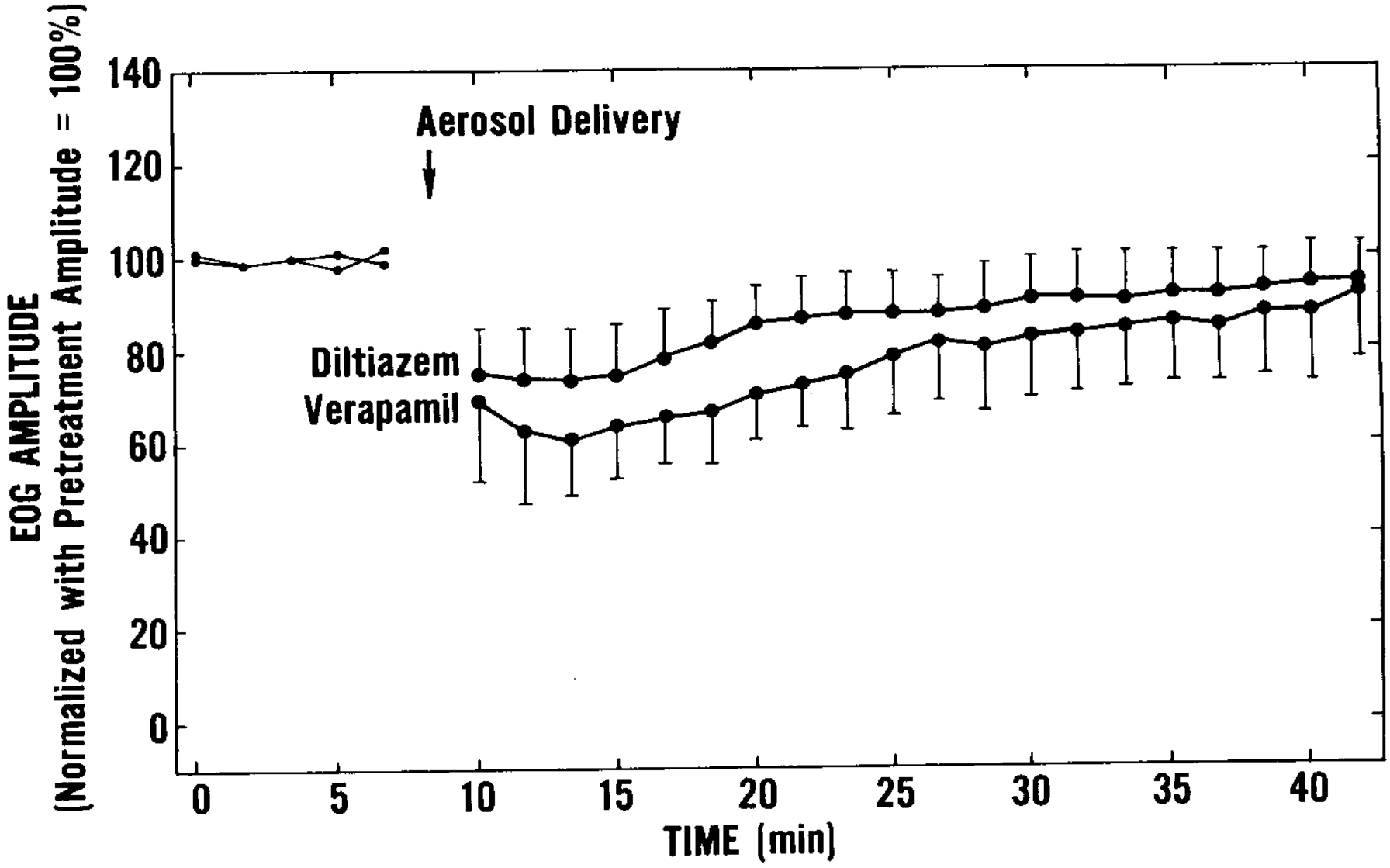
EOG AMPLITUDE
(Normalized with Pretreatment Amplitude = 100%)
140
120
100
80
60
40
20
0
Aerosol Delivery
Diltiazem
Verapamil
0
5
10
15
20
25
30
35
40
TIME (min)

Figure 11.

Bar graph of percent inhibition averaged over 33 min post-treatment. Diltiazem and verapamil were applied to give a calculated final concentration of 1.5 X 10^{-4}M. Distilled water is included as a control. Results are means +/- SD for the number of trials given in parentheses.

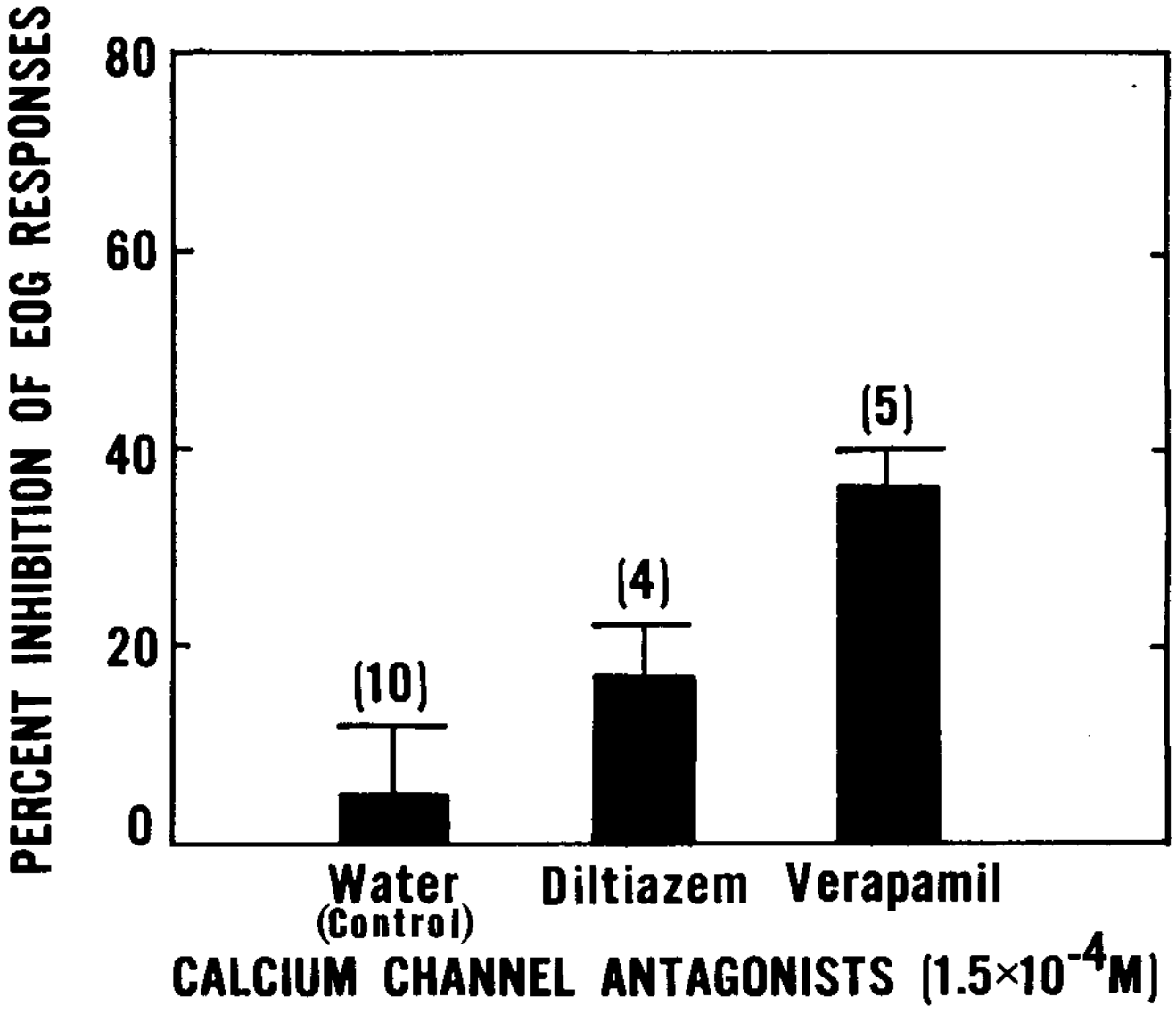
PERCENT INHIBITION OF EOG RESPONSES
80
60
40
20
0
(10)
(4)
(5)
Water
(Control)
Diltiazem
Verapamil
CALCIUM CHANNEL ANTAGONISTS (1.5×10-4M)

Figure 12.

Dose-response curve for diltiazem. Each point represents the mean +/- SD from four or more experiments.

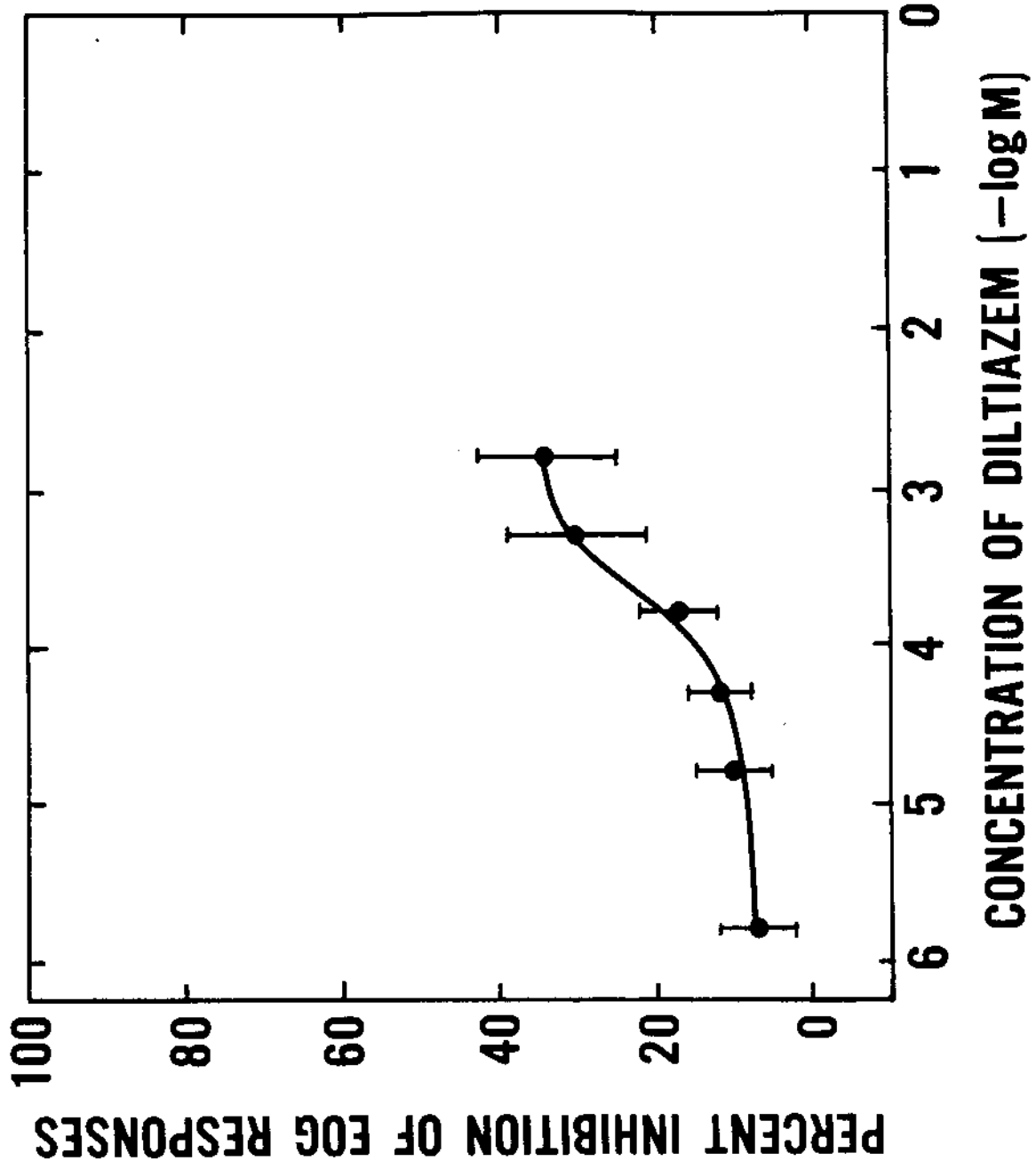
PERCENT INHIBITION OF EOG RESPONSES
100
80
60
40
20
0
6
5
4
3
2
1
0
CONCENTRATION OF DILTIAZEM (−log M)

Figure 13.

Dose-response curve for verapamil. Each point represents the mean +/- SD from four or more experiments.

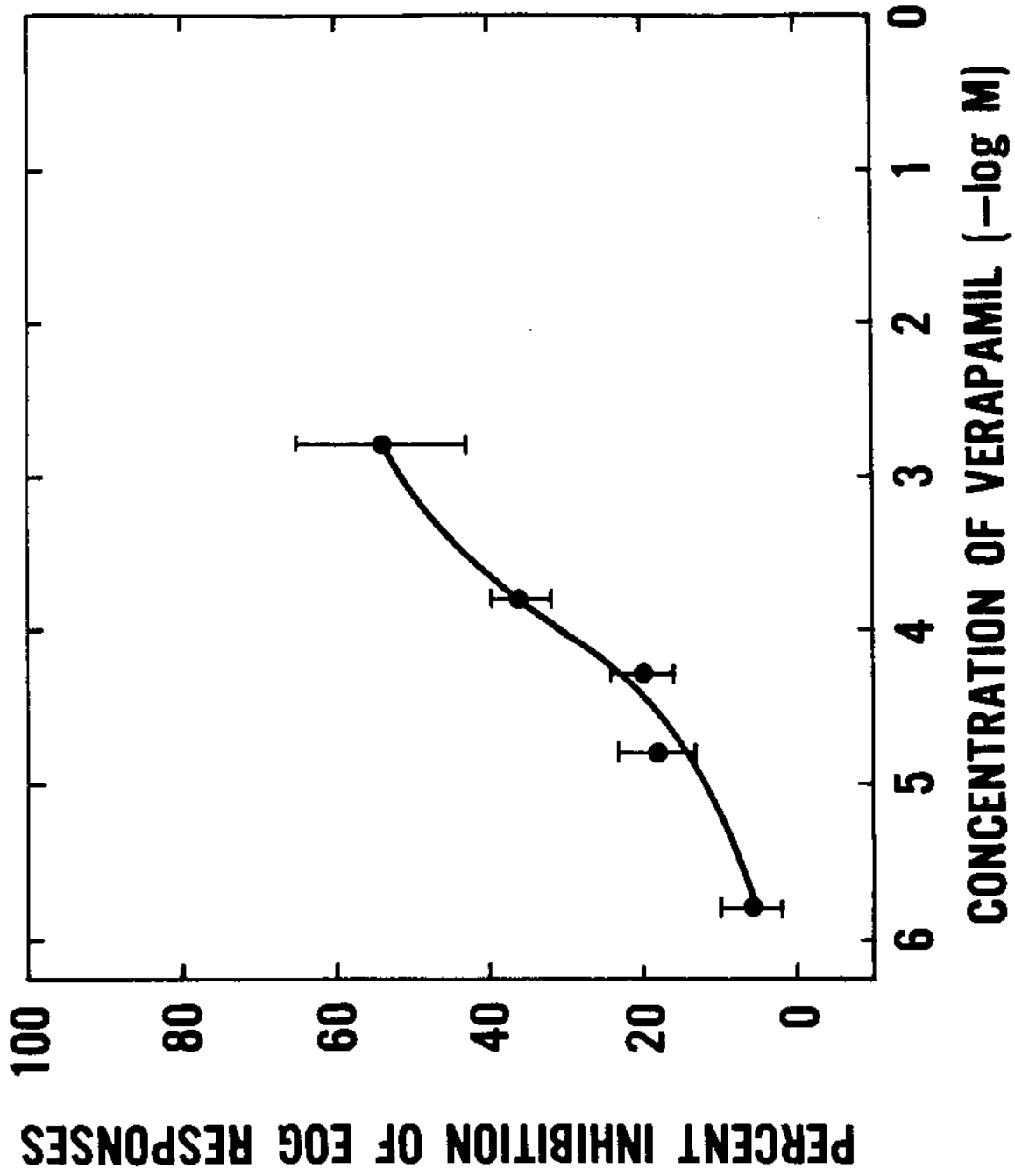
PERCENT INHIBITION OF EOG RESPONSES
100
80
60
40
20
0
6
5
4
3
2
1
0
CONCENTRATION OF VERAPAMIL (−log M)

Figure 14.

Averaged recovery curves following 2 sec aerosol sprays of nifedipine (N = 4) and nicardipine (N = 4) applied to give a calculated final concentration of 1.5 X 10^{-5}M. Both agents were dissolved in 1% DMSO, and the DMSO curve is a control (N = 7). Bars represent SD.

EOG AMPLITUDE
(Normalized with Pretreatment Amplitude = 100%)
140
120
100
80
60
40
20
0
0
5
10
15
20
25
30
35
40
TIME (Min)
Aerosol Delivery
1% DMSO
Nicardipine
Nifedipine

Figure 15.

Bar graph of percent inhibition averaged over 33 min post-treatment. Nicardipine and nifedipine were applied to give a calculated final concentration of 1.5×10^{-5} M One percent DMSO is included as a control. Results are means +/- SD for the number of trials given in parentheses.

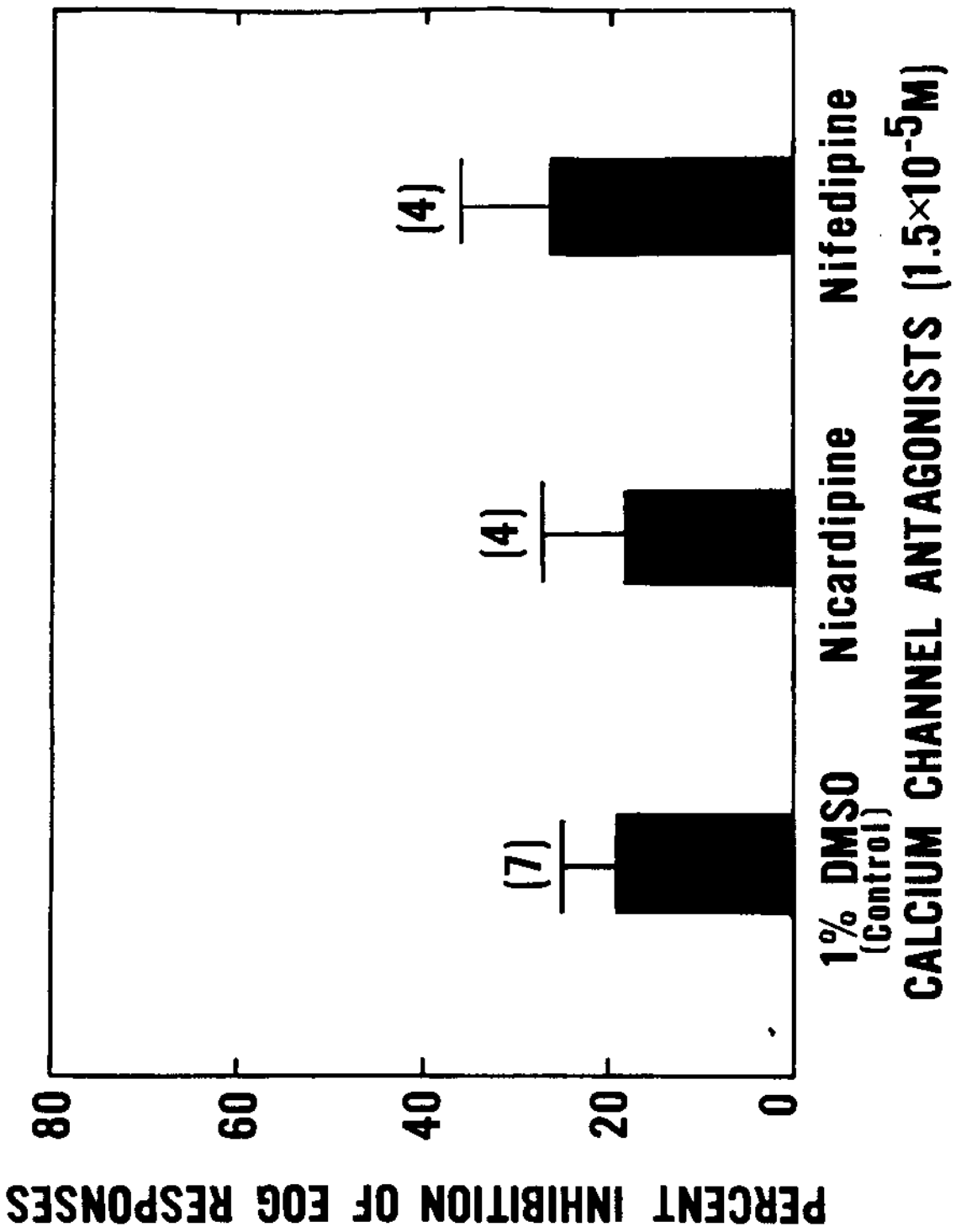
PERCENT INHIBITION OF EOG RESPONSES
80
60
40
20
0
(7)
(4)
(4)
1% DMSO
(Control)
Nicardipine
Nifedipine
CALCIUM CHANNEL ANTAGONISTS (1.5×10-5M)

Figure 16.

Averaged recovery curve following 2 sec aerosol sprays of W-7 (N = 7) applied to give a calculated final concentration of 1.5 X 10^{-5}M. W-7 was dissolved in 1% PEG 400, and the 1% PEG 400 curve is a control (N = 6). Bars represent SD.

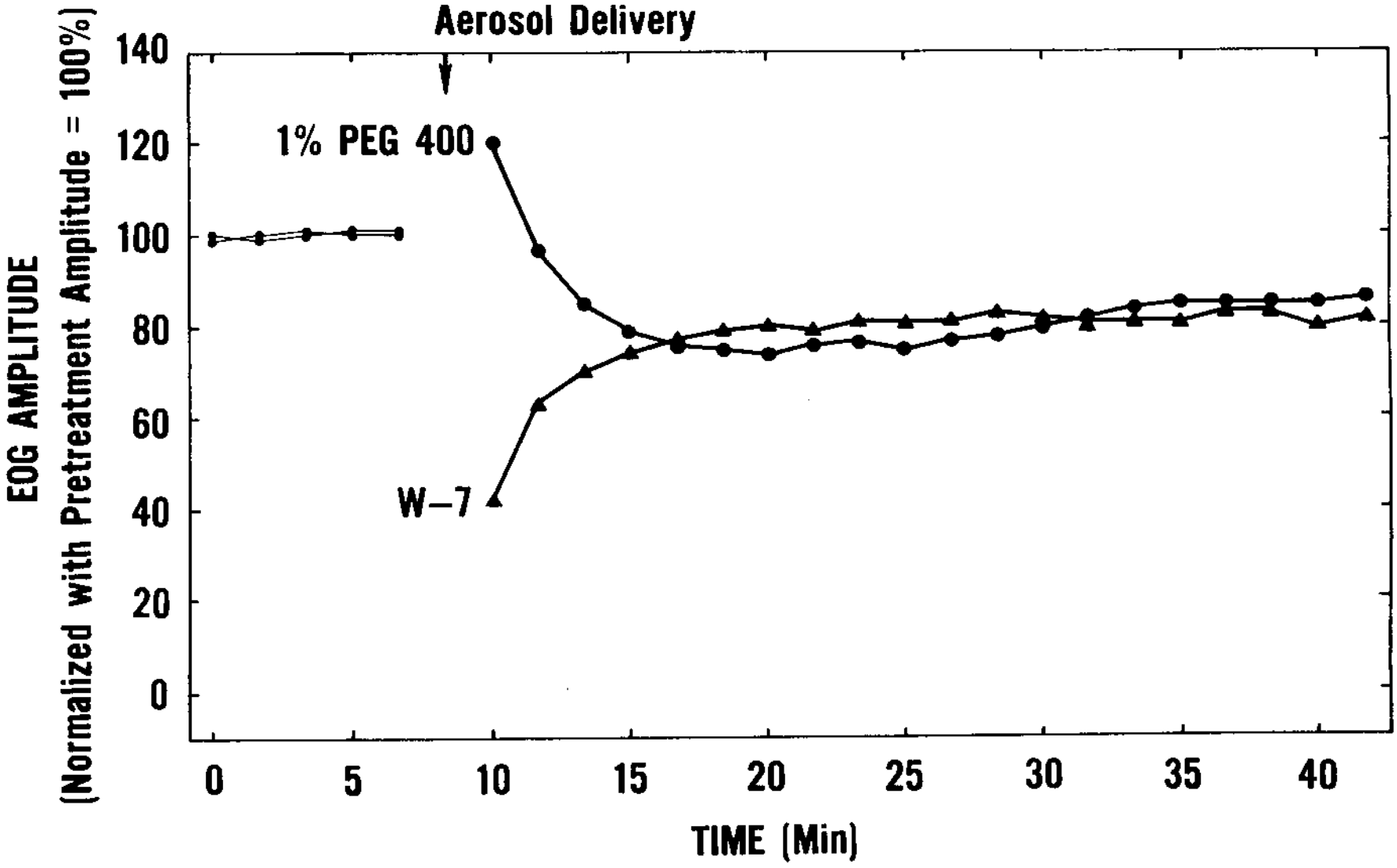
Aerosol Delivery
1% PEG 400
W–7
EOG AMPLITUDE
(Normalized with Pretreatment Amplitude = 100%)
140
120
100
80
60
40
20
0
0
5
10
15
20
25
30
35
40
TIME (Min)

Figure 17.

Averaged recovery curves following 2 sec aerosol sprays of chlorpromazine (N = 4) and trifluoperazine (N = 4). Both were applied to give a calculated final concentration of 1.5×10^{-4}M. Bars represent SD.

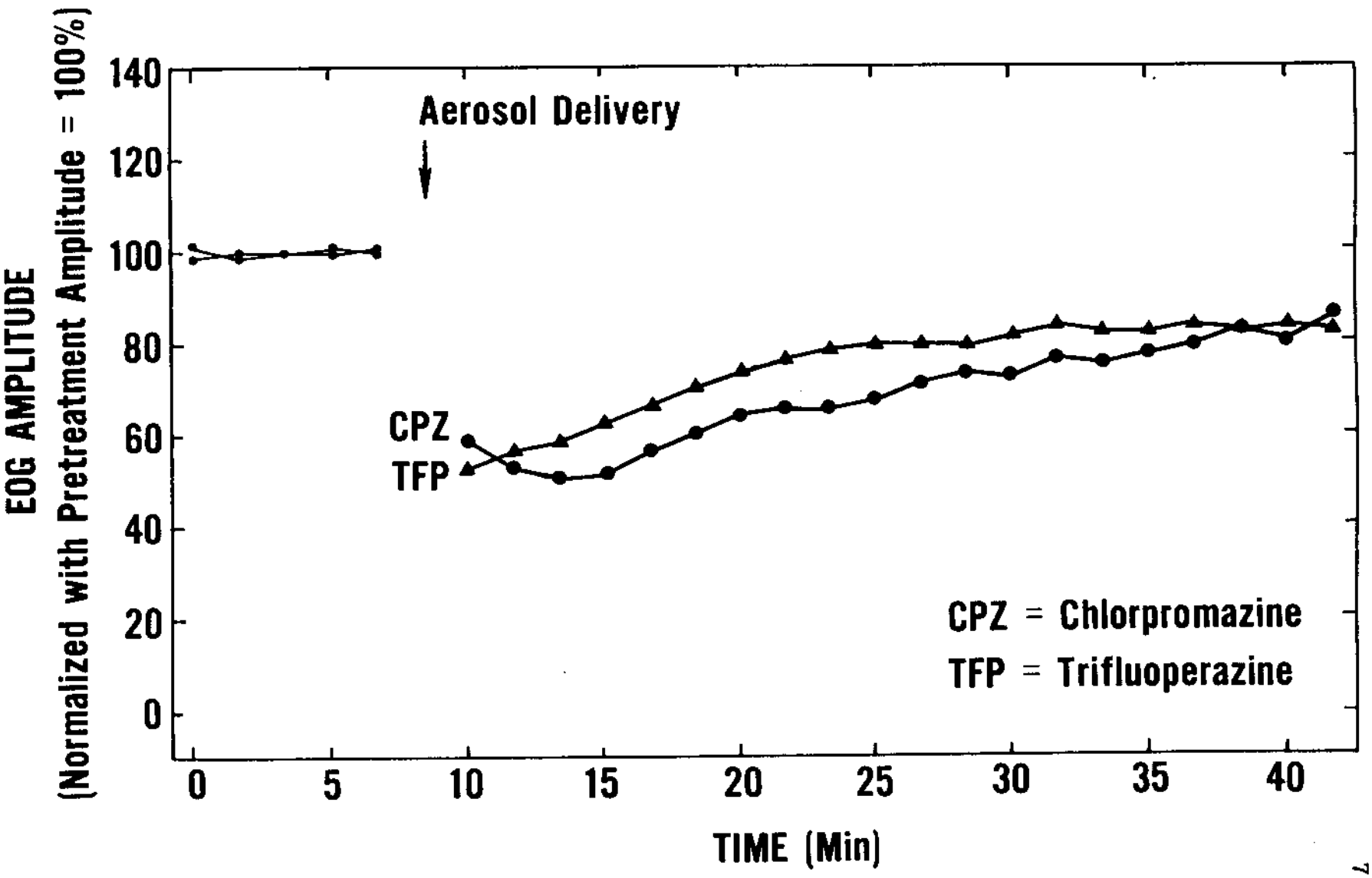
EOG AMPLITUDE
(Normalized with Pretreatment Amplitude = 100%)
140
120
100
80
60
40
20
0
Aerosol Delivery
CPZ
TFP
CPZ = Chlorpromazine
TFP = Trifluoperazine
0
5
10
15
20
25
30
35
40
TIME (Min)

Figure 18.

Bar graph of averaged percent inhibition averaged over 33 min post-treatment. Chlorpromazine (CPZ), trifluoperazine (TFP), and W-7 were applied to give a calculated final concentration of 1.5 X 10^{-4}M. One percent PEG 400 (used to dissolve W-7) and water are included as controls. Results are means +/- SD for the number of trials given in parentheses.

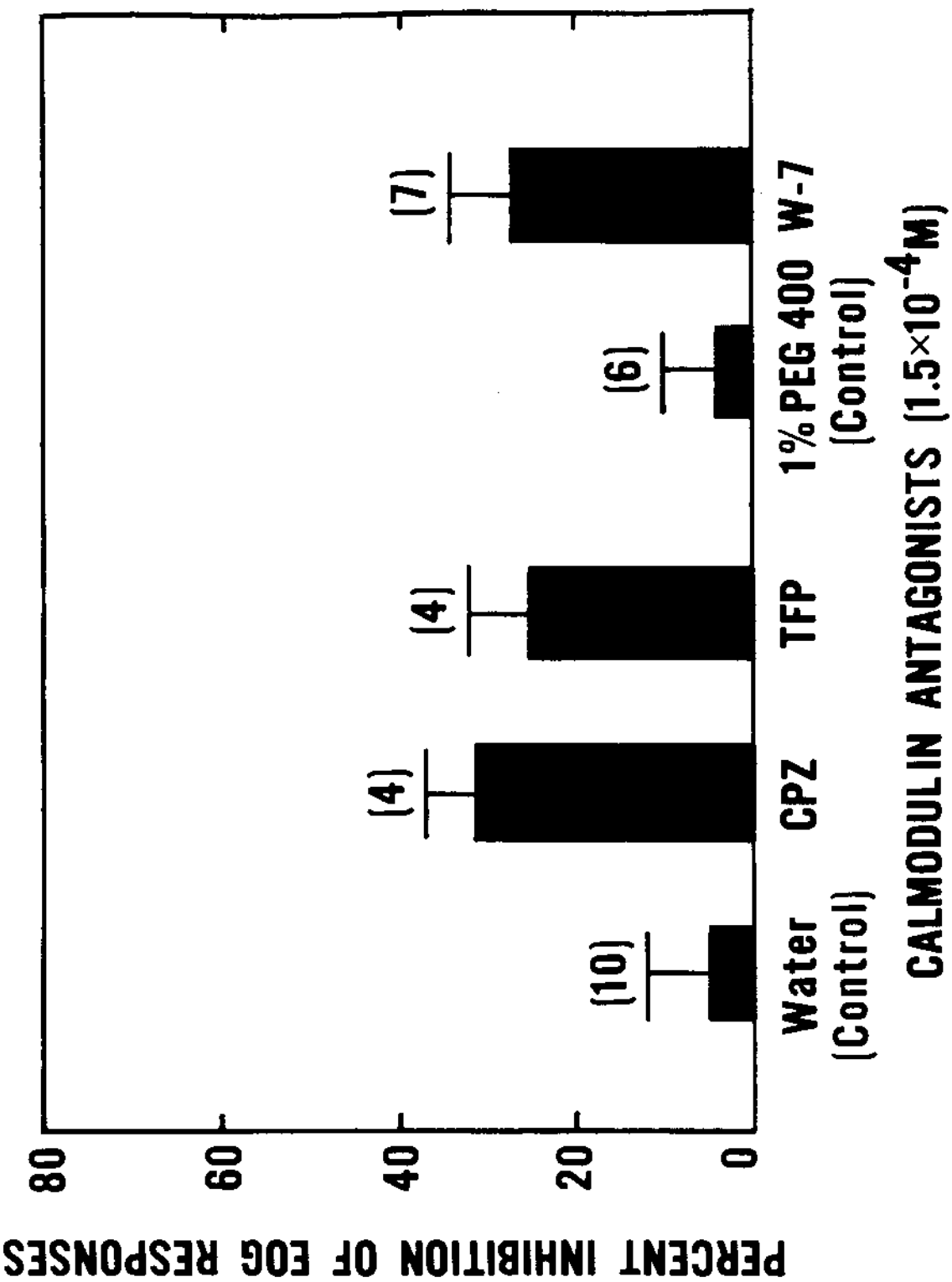
PERCENT INHIBITION OF EOG RESPONSES
0
20
40
60
80
(10)
(4)
(4)
(6)
(7)
Water (Control)
CPZ
TFP
1% PEG 400 (Control)
W-7
CALMODULIN ANTAGONISTS (1.5×10⁻⁴M)

Figure 19.

Averaged recovery curves following 2 sec aerosol sprays of cAMP (N = 4), dibutyryl cAMP (dbcAMP) (N = 4), cGMP (N = 4), and dibutyryl cGMP (dbcGMP) (N = 6). Adenosine is included as a control (N = 4). All agents were applied to give a calculated final concentration of 1.5 X 10^{-4}M. Bars represent SD.

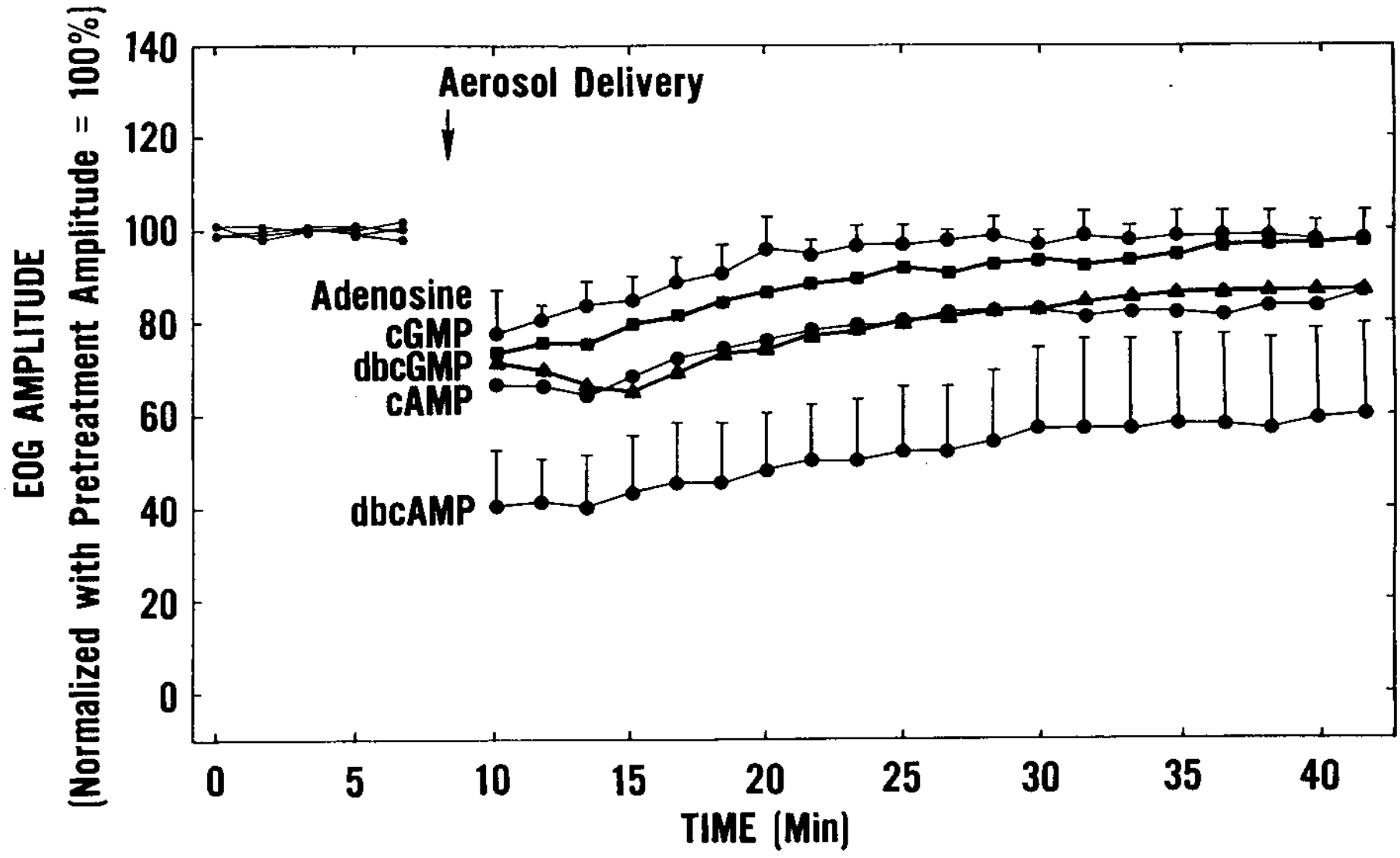
EOG AMPLITUDE
(Normalized with Pretreatment Amplitude = 100%)
140
120
100
80
60
40
20
0
Aerosol Delivery
Adenosine
cGMP
dbcGMP
cAMP
dbcAMP
0
5
10
15
20
25
30
35
40
TIME (Min)

Figure 20.

Bar graph of percent inhibition averaged over 33 min post-treatment. Adenosine, cAMP, cGMP, dbcAMP, and dbcGMP were applied to give a calculated final concentration of 1.5 X 10^{-4}M. Results are means +/- SD for the number of trials given in parentheses.

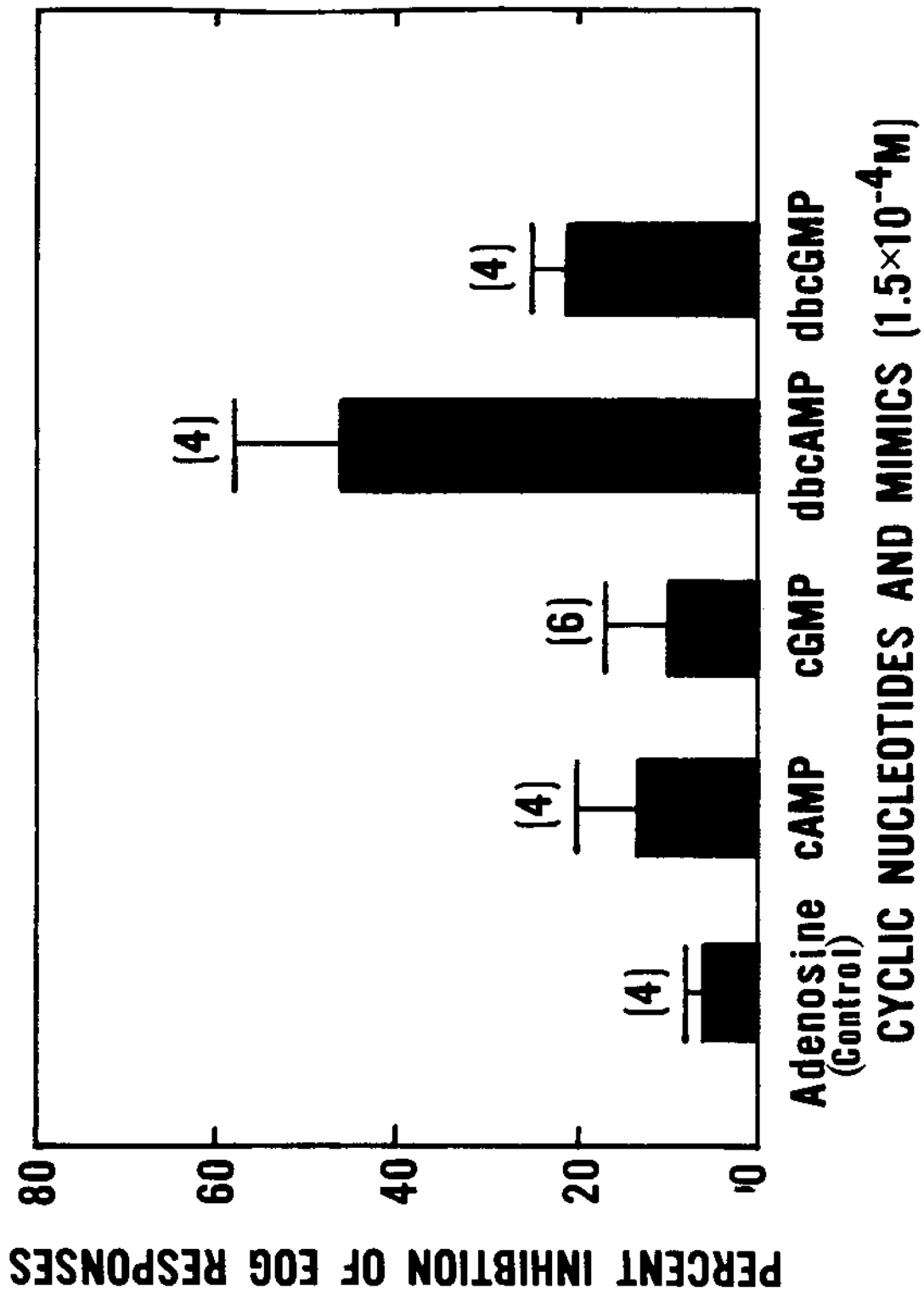
PERCENT INHIBITION OF EOG RESPONSES
0
20
40
60
80
(4)
(4)
(6)
(4)
(4)
Adenosine (Control)
cAMP
cGMP
dbcAMP
dbcGMP
CYCLIC NUCLEOTIDES AND MIMICS (1.5×10⁻⁴M)

Figure 21.

Averaged recovery curves following 2 sec aerosol sprays of forskolin to give a calculated final concentration of 1.5×10^{-5}M (N = 6). Forskolin was dissolved in 1% DMSO, and the DMSO curve is a control (N = 7). Bars represent SD.

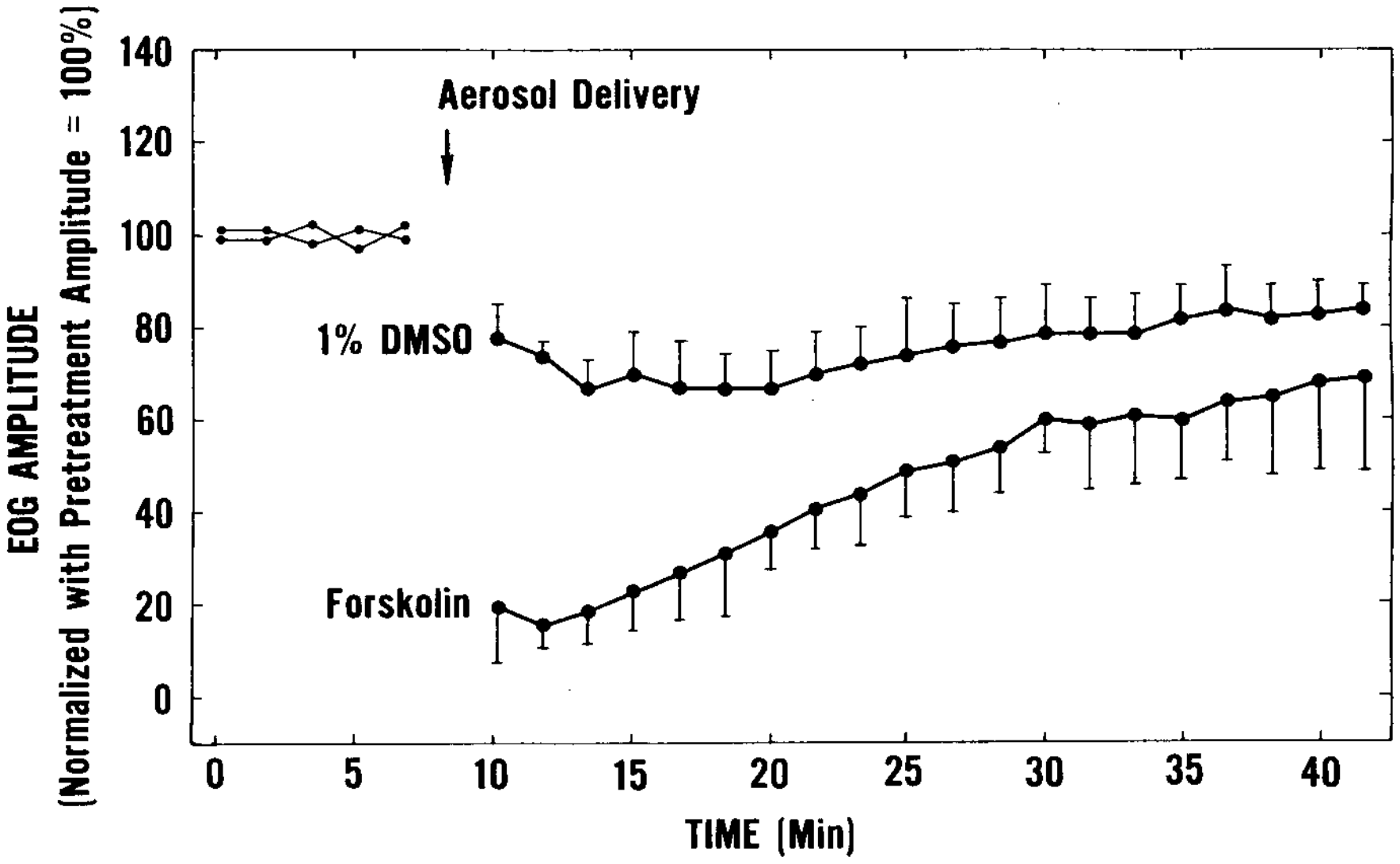
EOG AMPLITUDE
(Normalized with Pretreatment Amplitude = 100%)
140
120
100
80
60
40
20
0
Aerosol Delivery
1% DMSO
Forskolin
0
5
10
15
20
25
30
35
40
TIME (Min)

Figure 22.

Dose-response curve for forskolin. Each point represents the mean +/- SD from five experiments. The DMSO concentration was adjusted to 1% for each dilution.

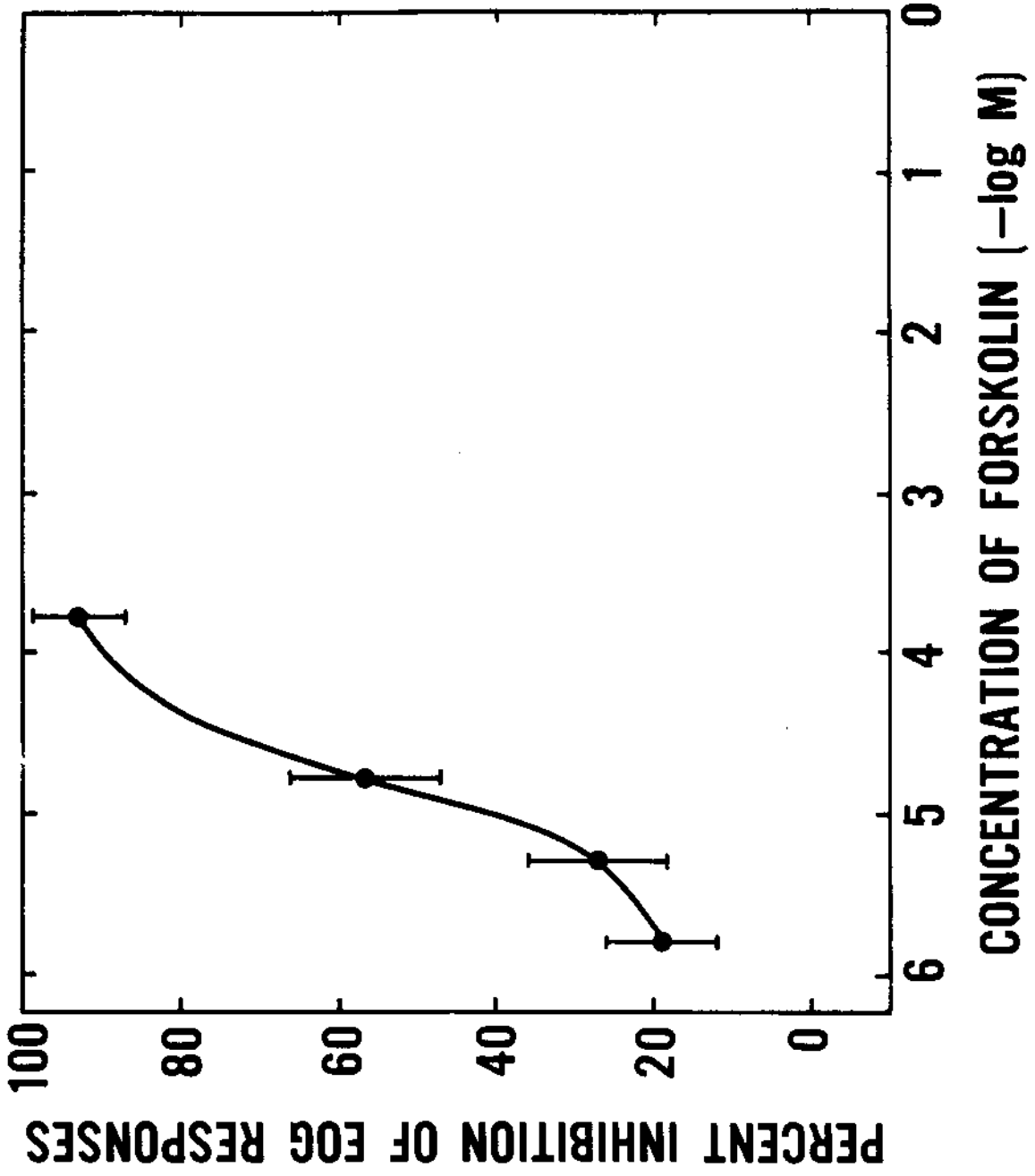
PERCENT INHIBITION OF EOG RESPONSES
100
80
60
40
20
0
6
5
4
3
2
1
0
CONCENTRATION OF FORSKOLIN (−log M)

CHAPTER IV

DISCUSSION

This study examined the role of Ca^{2+} as a current carrier and Ca^{2+}, cAMP, and other possible second messengers in olfactory transduction. The main technique used was aerosol application of agonists and antagonists onto the ventral olfactory mucosae of anesthetized frogs during electrophysiological recording of electroolfactogram (EOG) responses.

Current Carriers in Olfactory Transduction

The literature on olfaction is unclear as to the specific ions involved in the receptor potential of individual olfactory receptor neurons and their mass response recorded as the EOG (Kleene, 1986). It seems reasonable that sodium ions would be the main charge carriers for olfactory receptor potentials, by analogy with most other excitable tissues (Lancet, 1986), although Vodyanoy and Murphy (1983) and Dionne (1986) have obtained evidence for several types of K^+-selective channels in rat and mouse olfactory receptor neurons. Calcium ions appear to be required for receptor potential generation (Kleene, 1986)

but their specific role in olfactory transduction is not understood.

Effects of Inorganic Calcium Channel Blockers

The data reported in this study provide the most extensive evidence so far that Ca^{2+} is required for olfactory responses. Inorganic cations inhibit EOG responses in the frog in a rank order which is highly correlated with their calcium channel blocking effectiveness in other tissues (Table 2). An exception to this correlaton is Co^{2+} which is less inhibitory to EOG's than would be expected from its relative effectiveness in blocking calcium channels in other tissues. However, the EOG-enhancing effect of Ba^{2+} strengthens the argument for a current-carrying role of Ca^{2+}, because substitution of Ba^{2+} for Ca^{2+} often produces greater currents than Ca^{2+} in other tissues (Hagiwara and Ohmori, 1982; Hille, 1984). Thus, EOG blockade by inorganic channel blockers such as La^{3+} (Figure 8) and EOG enhancement by Ba^{2+} (Figure 7) support a role for Ca^{2+} as a current carrier in olfactory transduction.

In some tissues, elevated intracellular Ca^{2+} ($[Ca^{2+}]_i$) inactivates voltage-gated calcium channels (Reuter, 1983). Barium ions substitute well for Ca^{2+} as current carriers, but do not inactivate calcium channels (Hille, 1984). This

phenomenon could explain the EOG enhancement observed with Ba^{2+}, because Ba^{2+} entry should not influence $[Ca^{2+}]_i$ and therefore not produce calcium channel inactivation.

It may seem illogical that the application of Ca^{2+} itself results in inhibition of subsequent EOG's. A plausible explanation for this result is that extracellular Ca^{2+} in high concentration typically reduces membrane permeability through a membrane-stabilizing action (Webb, 1982). Membrane permeability decreases as Ca^{2+} binds to acidic phospholipids in the membrane, increasing the phase transition temperature and decreasing membrane fluidity (Housley and Stanley, 1982).

Another possible explanation of inhibition by Ca^{2+} itself is its effect on potassium channels. A common regulatory function of increasing $[Ca^{2+}]_i$ is the activation of calcium-dependent potassium channels which carry outward current to prevent prolonged depolarization of the membrane (Fishman and Spector, 1981). That Ba^{2+} may block K^+ currents (Armstrong and Taylor, 1980) suggests the possibility that EOG enhancement by Ba^{2+} application is the result of K^+ channel blockade. However, there was no EOG enhancement in the frog after aerosol application of 4-aminopyridine and quinine, drugs which block K^+ channels (DeCoursey et al., 1984b). Only slight EOG inhibition was observed with these agents in preliminary experiments at concentrations in the millimolar range (data not shown).

Effects of Organic Calcium Channel Antagonists

In these experiments, many of the organic calcium channel antagonists tested blocked EOG's to some extent. The dose-response curve for diltiazem (Figure 12) has a lower asymptotic limit than the dose-response curve for verapamil (Figure 13). This result suggests that these compounds differ in their intrinsic activity to inhibit EOG's. However, since the two curves overlap extensively, diltiazem and verapamil may have similar affinities for the binding sites which mediate EOG inhibition.

The 1,4-dihydropyridine, nifedipine, had little or no effect on EOG magnitude at a calculated final concentration of 1.5×10^{-5}M. Because nifedipine typically exerts physiological actions at a much lower concentration (e.g., 10^{-9}M; Miller, 1985), it seems likely the receptor neurons lack binding sites for this class of calcium channel antagonists. Inhibition of EOG's by diltiazem and verapamil, but not by 1,4-dihydropyridines, follows the pharmacological profile of so-called N-type calcium channels.

Of the various known types of calcium channels, N-type channels are found on sensory neurons and are characterized by insensitivity to 1,4-dihydropyridines (Reuter, 1985). Additional evidence for involvement of N-type calcium channels in olfaction is that the N-type channels are known

to be blocked by Cd^{2+}, but enhanced by Ba^{2+} (Nowycky et. al., 1985). In this study, EOG's were inhibited by Cd^{2+} and enhanced by Ba^{2+}. By contrast, T-type calcium channels are resistant to Cd^{2+} blockade and 1,4-dihydropyridines while being equally permeable to Ca^{2+} and Ba^{2+} (Nilius et al., 1985). Yet another category, the L-type calcium channels, are susceptible to blockade by 1,4-dihydropyridines (Reuter, 1985). Collectively, the EOG data suggest a pharmacological profile characteristic of N-type calcium channels.

Calmodulin and Cyclic AMP in Olfactory Transduction

Calmodulin

In these experiments, calmodulin antagonists inhibited EOG's, but not in a rank order which corresponds to their known binding affinities for calmodulin. Trifluoperazine (TFP) has a greater affinity for calmodulin than chlorpromazine (CPZ) (Levin and Weiss, 1979), but CPZ inhibited EOG's more than TFP (Figure 18). Inhibition of EOG's by CPZ and TFP may result from non-specific membrane effects rather than anti-calmodulin activity. Both CPZ and TFP are cationic, amphipathic agents. Because each possesses a hydrophobic region plus a nitrogen atom which can acquire a positive charge, these compounds can partition into and

disrupt hydrophobic regions of protein and lipid in the cell membrane (Landry et al., 1981; Lieber et al., 1984). For example, CPZ can cause invaginations of red blood cell membranes, possibly by differentially expanding the negatively charged cytoplasmic face of the bilayer (Lieber et al., 1984).

Inhibition of EOG's by the calmodulin antagonist W-7 suggests a role for calmodulin in olfactory transduction (Figure 16). However, W-7 is a relatively new compound which may have undefined nonspecific effects. The CPZ and TFP results argue against a role of calmodulin in olfactory transduction, although the effects of W-7 deserve further study. Both CPZ and TFP inhibit protein kinase C (Schatzman et al., 1981), which is activated by diacylglycerol (Michell, 1983). Thus further research is needed to understand whether inositol phospholipids, as well as calmodulin, are second messengers in olfactory transduction.

Cyclic AMP

According to Lancet (1986), all of Sutherland's criteria (Robinson et al., 1971) for cAMP involvement as a second messenger in olfactory transduction have been met. The inhibition of EOG's by dbcAMP (a cAMP mimic) and forskolin (an adenylate cyclase activator) in these studies

supports the hypothesis of cAMP involvement in olfactory transduction. Since dbcAMP and forskolin attenuate EOG responses to odorants, an inhibitory role is implied. Inhibitory action by cAMP is not without precedent. For example, cAMP seems to mediate the hyperpolarizing action of norepinephrine (NE) in cerebellar and hippocampal neurons (Drummond, 1984). Application of NE onto rat hippocampal slices increases cAMP levels three- to fourfold and hyperpolarizes CA1 neurons (Segal et al., 1981).

Cyclic AMP could be involved in sensory adaptation, a process which has been compared to receptor desensitization (Lancet, 1986). Desensitization results from either a decreased response during continued agonist exposure, or with repeated applications of the same agonist (Hollenberg, 1985). Desensitization may involve changes in the state of the receptor or changes at other sites such as ion channels (Richards, 1983), with mediation through protein phosphorylation (Ewald et al., 1985). Apropos of this study, Siegelbaum et al. (1982) have demonstrated that cAMP closes K^+ channels in Aplysia sensory neurons, leading to hyperpolarization. In a model proposed by Lancet (1986), ion channels are suggested as possible target sites for cAMP-mediated protein phosphorylation and regulation of the membrane potential.

Summary

1. Inhibition of EOG's by inorganic calcium channel blockers and organic calcium channel antagonists supports a role for Ca^{2+} in olfactory transduction.

2. The inorganic cations inhibit EOG's in a rank order and concentration consistent with calcium channel blockade in other tissues.

3. The EOG enhancement observed with the application of Ba^{2+} supports a role for Ca^{2+} as a charge carrier in olfactory transduction, based on the effect of Ba^{2+} in other tissues.

4. Calcium ion could also serve as an intracellular second messenger, although a role for calmodulin was not strongly supported in this study.

5. The lipophilic cAMP mimic, dbcAMP, and the adenylate cyclase activator, forskolin, are both effective EOG inhibitors, suggesting that increased cAMP levels in olfactory receptor neurons reduces EOG amplitudes.

6. Cyclic AMP could be involved with the primary excitatory process or sensory adaptation, or both.

7. Possible roles of cAMP include mediating functional changes in transduction mechanisms, perhaps by phosphorylation of ion channels to produce opening or closing of the channels.

BIBLIOGRAPHY

Adamek, G.D., R.C. Gesteland, R.G. Mair, and B. Oakley 1984 Transduction physiology of olfactory receptor cilia. Brain Research, 310, 87-98.

Adams, W.B. and I.B. Levitan 1982 Intracellular injection of protein kinase inhibitor blocks the serotonin-induced increase in K^+ conductance in Aplysia neuron R15. Proceedings of the National Academy of Sciences, USA, 79, 3877-3880.

Anholt, R.R.H., K.M.M. Murphy, G.E. Mack, and S.H. Snyder 1984 Peripheral-type benzodiazepine receptors in the central nervous system: localization to olfactory nerves. Journal of Neurosciences, 4, 593-603.

Armstrong, C.M. and S.R. Taylor 1980 Interaction of barium ions with potassium channels in squid giant axons. Biophysical Journal, 30, 473-488.

Arvidson, B. 1981 Is cadmium toxic to the nervous system? Trends in Neuroscience, 4, XI-XIV.

Barber, V.C. 1974 Cilia in sense organs. In M.A. Sleigh (ed.), Cilia and Flagella. Academic Press, New York.

Brostrom, C.O., Y.-C. Huang, B.McL. Breckenridge, and D.J. Wolff 1975 Identification of a calcium-binding protein as a calcium dependent regulator of brain adenylate cyclase. Proceedings of the National Academy of Sciences, USA, 72, 64-68.

Chau, V., C.Y. Huang, P.B. Chock, J.H. Wong, and R.K. Sharma 1982 Kinetic studies of the activation of cyclic nucleotide phosphodiesterase by Ca^{2+} and calmodulin. In S. Kakiuchi, H. Hidaka, and A.R. Means (eds.), Calmodulin and Intracellular Ca^{2+} Receptors. Plenum Press, New York.

Cheung, W.Y. 1970 Cyclic nucleotide phosphodiesterase. In P. Greengard and E. Costa (eds.), Role of Cyclic AMP in Cell Function. Advances in Biochemical Psychopharmacology, Volume 3. Raven Press, New York.

Cohen, P. 1982 The role of protein phosphorylation in neural and hormonal control of cellular activity. Nature, 296, 613-620.

DeCoursey, T.E., K.G. Chandy, S. Gupta, and M.D. Cahalan 1984a Pharmacology of human T lymphocyte K channels. Biophysical Journal, 45, 144a.

DeCoursey, T.E., K.G. Chandy, S. Gupta, and M.D. Cahalan 1984b Voltage-gated K^+ channels in human T lymphocytes: a role in mitogenesis? Nature, 307, 465-468.

Depeyer, J.E., A.B. Cachelin, I.B. Levitan, and H. Reuter 1982 Ca^{2+} activated K^+ conductance in internally perfused snail neurons is enhanced by protein phosphorylation. Proceedings of the National Academy of Sciences, USA, 79, 4207-4211.

DeSimone, J.A. 1981 Physicochemical principles in taste and olfaction. In R.H. Cagan and M.R. Kare (eds.), Biochemistry of Taste and Olfaction. Academic Press, New

York.

Dionne, V.E. 1986 Membrane conductance mechanisms in dissociated cells from the necturus olfactory epithelium. International Symposium on Olfaction and Taste Abstracts, S45.

Drummond, G. I. 1984 Cyclic nucleotides in the nervous system. Raven Press, New York.

Ehlert, F.J., W.R. Roeska, E. Itoga, and H. Yamamura 1982 The binding of [3H]nitrendipine to receptors for calcium channel antagonists in the heart, cerebral cortex, and ileum of rats. Life Sciences, 30, 2191-2202.

Ewald, D.A., A. Williams, and I.B. Levitan 1985 Modulation of single Ca^{2+}-dependent K^{+}-channel activity by protein phosphorylation. Nature, 315, 503-506.

Fisher, S., L.A.A. Van Rooijen, and B.W. Agranoff 1984 Renewed interest in the polyphosphoinositides. Trends in Biochemical Sciences, 9, 53-56.

Fishman, M.C. and I. Spector 1981 Potassium current supression by quinidine reveals additional calcium currents in neuroblastoma cells. Proceedings of the National Academy of Sciences, USA, 78, 5245-5249.

Fuortes, M.G.F. 1971 Generation of responses in receptor. In W.R. Lowenstein (ed), Handbook of Sensory Physiology, Vol. 1. Springer-Verlag, New York. 243.

Garcia, M.L., V.F. King, P.K.S. Siegl, J.P. Reuben, and G.J. Kaczorowski 1986 Binding of Ca^{2+} entry blockers to cardiac

sarcolemmal membrane vesicles. The Journal of Biological Chemistry, 261(18), 8146-8157.

Gestelend, R.C. 1964 Initial events of the electroolfactogram. Annals of the N.Y. Academy of Sciences, 116, 440-447.

Gesteland, R., J. Lettvin, and W. Pitts 1965 Chemical transmission in the nose of the frog. Journal of Physiology, 181, 525-559.

Getchell, T.V., G.L. Heck, J.A. DeSimone, and S. Price 1980 The location of olfactory receptor sites: inferences from latency measurements, Biophysical Journal, 29, 397-411.

Glossmann, H., D.R. Ferry, F. Lubbecke, R. Mewes, and F. Hofmann 1982 Calcium channels: direct identification with radioligand binding studies. Trends in Pharmacological Sciences, 3, 431-437.

Graziadei, P.P.C. 1973 The ultrastructure of vertebrates olfactory mucosa. In Friedmann (ed.), The Ultrastructure of Sensory Organs. North-Holland Publishing Company, New York.

Graziadei, P.P.C. and G.A.M. Graziadei 1976 Olfactory epithelium of Necturus maculosus and Ambystoma tigrinum. Journal of Neurocytology, 5, 11-32.

Hagiwara, S. and K. Takahashi 1967 Surface density of calcium ions and calcium spikes in the barnacle muscle fiber membrane. Journal of General Physiology, 50, 583-601.

Hagiwara, S. and Ohmori 1982 Studies of calcium channels in rat clonal pituitary cells with patch electrode voltage clamp. Journal of Physiology (London), 331, 231-252.

Hagiwara, S. and L. Byerly 1983 The calcium channel. Trends in Neuroscience, 6, 189-193.

Hays, W.L. 1981 Statistics (third edition). Holt, Rinehart and Winston, New York.

Hess, P. and R.W. Tsien 1984 Mechanism of ion permeation through calcium channels. Nature, 309, 453-456.

Hidaka, H. and T. Tanaka 1982 Biopharmacological assessment of calmodulin function: utility of calmodulin antagonists. In S. Kakiuchi, H. Hidaka, and A.R. Means (eds.), Calmodulin and Intracellular Ca^{2+} Receptors. Plenum Press, New York.

Hille, B. 1984 Ionic Channels of Excitable Membranes. Sinauer Associates Inc., Sunderland, Massachusetts.

Hinds, W.C. 1982 Aerosol Technology. John Wiley and Sons, New York.

Hirsch, J.D. and F.L. Margolis 1981 Isolation, separation, and analysis of cells from olfactory epithelium. In R.H. Cagan and M.R. Kare (eds), Biochemistry of Taste and Olfaction. Academic Press, New York.

Hollenberg, M.D. 1985 Receptor models and the action of neurotransmitters and hormaones: some new perspectives. In H.I. Yamamura, S.J. Enna, and M.J. Kuhar (eds.), Neurotransmitter Receptor Binding. Raven Press, New York.

Houslay, M.D. and K.K. Stanley 1982 Dynamics of Biological Membranes: Influences on Synthesis, Structure and Function. John Wiley and Sons, New York.

Hurwitz, L. 1986 Pharmacology of calcium channels and smooth muscle. Annual Review of Pharmacology and Toxicology, 26, 225-258.

Janis, R.A. and D.J. Triggle 1984 1,4-Dihydropyridine Ca^{2+} channel antagonists and activators: a comparison of binding characteristics with pharmacology. Drug Development Research, 4, 257-274.

Karlin, A. 1983 The anatomy of a receptor. Neuroscience Commentaries, 1, 111-123.

Kleene, S.J. 1986 Bacterial chemotaxis and vertebrate olfaction. Experientia, 42, 241-250.

Kurihara, K. and N. Koyama 1974 High activity of adenyl cyclase in olfactory and gustatory organs. Biochemica Biophysica Acta, 421, 380-394.

Lancet, D. 1986 Vertebrate olfactory reception. Annual Review of Neuroscience, 9, 329-355.

Landry, Y., A. and M. Ruckstuhl 1981 Can calmodulin inhibitors be used to probe calmodulin effects? Biochemical Pharmacology, 30, 2031-2032.

Lansman, J.B., P. Hess, and R.W. Tsien 1985 Direct measurement of entry and exit rates for calcium ions in single calcium channels. Biophysical Journal, 47, 67a.

Law, J.S. and R.I. Henkin 1982 Taste bud adenosine -3'5'-monophosphate phosphodiesterase: activity, subcellular distribution and kinetic parameters. Research Communications in Chemical Pathology and Pharmacology, 38, 439-452.

Lee, K.S. and R.W. Tsien 1983 Mechanism of calcium channel blockade by verapamil, D600, diltiazem and nitrendipine in single dialysed heart cells. Nature, 302, 790-794.

Leslie, S.W., E. Barr, J. Chandler, and R.P. Farrar 1983 Inhibition of fast- and slow-phase depolarization dependent synaptosomal calcium uptake by ethanol. Journal of Pharmacology and Experimental Therapeutics, 225, 571-575.

Leslie, S.W., J.J. Woodward, R.E. Wilcox, and R.P. Farrar 1986 Chronic ethanol treatment uncouples striatal calcium entry and endogenous dopamine release. Brain Research, in press.

Levin, R.M., and B. Weiss 1976 Mechanism by which psychotropic drugs inhibit adenosine cyclic 3'5'-monophosphate phosphodiesterase of brain. Molecular Pharmacology, 12, 581-589.

Levin, R.M. and B. Weiss 1979 Selective binding of antipsychotics and other psychoactive agents to the calcium-dependent activator of cyclic nucleotide phosphodiesterase. The Journal of Pharmacology and Experimental Therapeutics, 208, 454-459.

Levitan, I.B., J.R. Lemos, and I. Novak-Hofer 1983 Protein phosphorylation and the regulation of ion channels. Trends in Neurosciences, 6, 496-499.

Libet, B. 1967 Long latent periods and further analysis of slow synaptic responses in sympathetic ganglia. Journal of Neurophysiology, 30, 494-514.

Libet, B. 1970 Generation of slow inhibitory and excitatory postsynaptic potentials. Federation Proceedings, 29, 1945-1956.

Lidow, M.S., B.Ph.M. Menco, R.C. Gesteland and A.I. Farbman 1983 Studies on the structure of the axoneme of olfactory cilia in frogs and rats using tannic acid-supplemented fixation and photographic rotation. Society for Neuroscience Abstracts, 9, part 2, 1019.

Lieber, M.R., Y. Lange, R.S. Weinstein, and T.L.Steck 1984 Interaction of chlorpromazine with the human erythrocyte membrane. The Journal of Biological Chemistry, 259, 9225-9234.

Madison, D.V. and R.A. Nicoll 1982 Noradrenaline blocks accomodation of pyramidal cell discharge in the hippocampus. Nature, 299, 636-638.

Menco, B.P.M., G.H. Dodd, M. Davey, and L.H. Bannister 1976 Presence of membrane particles in freeze-etched bovine olfactory cilia. Nature, 263, 597-599.

Menevse, A., G.H. Dodd, M. Poynder, and D. Squirrell 1977 A chemical modification approach to the olfactory code.

Biochemical Society Transactions, 5, 191-194.

Michell, R.H. 1983 Ca^{++} and protein kinase C: two synergistic cellular signals. Trends in Biochemical Sciences, 8, 263-265.

Miller, R.J. and S.B. Freedman 1984 Are dihydropyridine binding sites voltage sensitive calcium channels? Life Sciences, 34, 1205-1221.

Miller, R.J. 1985 How many types of calcium channels exist in neurones? Trends in Neurosciences, 8, 45-47.

Naitoh, Y. and R. Eckert 1974 The control of ciliary activity in Protozoa. In M.A. Sleigh (ed.), Cilia and Flagella. Academic Press, New York.

Nilius, B., P. Hess, J.B. Lansman, and R.W. Tsien 1985 A novel type of cardiac calcium channel in ventricular cells. Nature, 316, 443-446.

Nishizuka, Y. 1984 Turnover of inositol phospholipids and signal transduction. Science, 225, 1365-1370.

Nowycky, M.C., A.P. Fox, and R.W. Tsien 1985 Three types of neuronal calcium channel with different calcium agonist sensitivity. Nature, 316, 440-443.

Ottoson, D. 1956 Analysis of the electrical activity of the olfactory epithelium. Acta Physiologica Scandanavia, 35, suppl. 122, 1-83.

Pace, U., E. Hanski, Y. Salomon, and D. Lancet 1985 Odorant-sensitive adenylate cyclase may mediate olfactory reception. Nature, 316, 255-258.

Reese, T.S. 1965 Olfactory cilia in the frog. The Journal of Cell Biology, 25, 209-230.

Reuter, H. 1983 Calcium channel modulation by neurotransmitters, enzymes, and drugs. Nature, 301, 569-574.

Reuter, H. 1985 A variety of calcium channels. Nature, 316, 391.

Rhein, L.D. and R.H. Cagan 1980 Biochemical studies of olfaction: isolation, characterization, and odorant binding activity of cilia from rainbow trout olfactory resettes. Proceedings of the National Academy of Sciences, USA, 77, 4412-4416.

Richards, W.G. 1983 Quantum Pharmacology, second edition. Butterworths, London.

Robinson, G.A., R.W. Butcher, and E.W. Sutherland 1971 Cyclic AMP. Academic Press, New York.

Rosenberg, R.L., P. Hess, J.P. Reeves, H. Smilowitz, and R.W. Tsien 1986 Calcium channels in planar lipid bilayers: insights into mechanisms of ion permeation and gating. Science, 231, 1564-1566.

Schafer, R., D.W. Criswell, S.P. Fracek, Jr., and K.R. Brower 1984 Olfactory studies using ethyl bromoacetate and other chemically active odorants. Chemical Senses, 9, 31-52.

Schafer, R. J.C. Dickens, and S.P. Fracek, Jr. 1986a Inhibition of protein synthesis does not block

physiological responses to odors over the short term. Journal of Comparative Biochemistry and Physiology, in press.

Schatzman, R.C., B.C. Wise, and J.F. Kuo 1981 Phospholipid-sensitive calcium-dependent protein kinase: inhibition by antipsychotic drugs. Biochemical and Biophysical Research Communications, 98, 669-676.

Seamon, K. and J.W. Daly 1981 Activation of adenylate cyclase by the diterpine forskolin does not require the guanine nucleotide regulatory protein. The Journal of Biological Chemistry, 256, 9799-9801.

Segal, M., V. Greenberger, and R. Hofstein 1981 Cyclic AMP-generating systems in rat hippocampal slices. Brain Research, 213, 351-364.

Shepherd, G.M. 1974 The Synaptic Organization of the Brain. Oxford University Press, New York.

Shepherd, G.M., and B. Hedlund 1983 Muscarinic receptor-olfactory receptor interactions in the salamander olfactory epithelium. Society for Neuroscience Abstracts, 9, part 1, 463.

Siegelbaum, S.A., J.S. Camardo, and E.R. Kandel 1982 Serotonin and cyclic AMP close single K^+ channels in Aplysia sensory neurones. Nature, 299, 413-417.

Silver, W.L. and J.A. Maruniak 1981 Trigeminal chemoreception in the nasal and oral cavities. Chemical Senses, 6, 295-305.

Suzuki, N. 1978 Effects of different ionic environments on the responses of single olfactory receptors in the lamprey. Comparative Biochemistry and Physiology, 61, 461-467.

Takagi, S.F., H. Kitamura, K. Imai, and H. Takeuchi 1969 Further studies on the roles of sodium and potassium in the generation of the electro-olfactogram. Journal of General Physiology, 53, 115-130.

Takai, Y., K. Kaibuchi, T. Matsubara, K. Sana, Yu Nishizuka, and Y. Nishizuka 1982 Two transmembrane control mechanisms for protein phosphorylation in bidirectional regulation of cell functions. In S. Kakiuchi, H. Hidaka, and A.R. Means (eds.), Calmodulin and Intracellular Ca^{++} Receptors. Plenum Press, New York.

Vincenzi, F.F. 1982 The pharmacology of calmodulin antagonism: a reappraisal. In S. Kakiuchi, H. Hidaka, and A.R. Means (eds.), Calmodulin and Intracellular Ca^{++} Receptors. Plenum Press, New York.

Vodyanoy, V. and R.B. Murphy 1983 Single-channel fluctuations in bimolecular lipid membranes induced by rat olfactory epithelial homogenates. Science, 220, 717-719.

Webb, R.C. 1982 D-600 and the membrane stabilizing effect of calcium in vascular smooth muscle. Pharmacology, 25, 250-261.